Electronic Supplementary Material (ESI) for New Journal of Chemistry.
This journal is © The Royal Society of Chemistry and the Centre National de la Recherche Scientifique 2022

From methylarenes to Esters: Efficient oxidative Csp^3-H activation promoted by CuO decorated magnetic reduced graphene oxide

Dariush Khalili,*[1], Marzieh Rousta,[1] and Ali Khalafi-Nezhad[1], Edris Ebrahimi

[1]Department of Chemistry, College of Sciences, Shiraz University, Shiraz 71467-13565, Iran

Table of content

General

All chemicals used in this study were analytical grade, commercially available and used without further purification. Graphite (CAS No. 7782-42-5, particle size: <50μm) was purchased from Merck. Most of the products were purified by column chromatography from appropriate solvents and were identified by ^{1}H NMR and ^{13}C NMR. Progress of the reactions was monitored by TLC using silica gel polygrams SIL G/UV 254 plates. FT-IR spectra were recorded on Shimadzu DR-8001 Spectrometer and employed for characterization of the catalysts. NMR spectra were recorded on a Bruker Avance DPX 400 MHz Instrument in $CDCl_3$ or DMSO-*d6* solvents using TMS as internal standard. Chemical shifts were reported in ppm (δ), and coupling constants (J), in Hz. X-ray diffraction (XRD) patterns were recorded on a XRD-D8 (BRUKER, Germany) employing a scanning rate of 0.05° s^{-1} from 10° to 80° with Cu$K\alpha$ radiation. The surface morphology of graphene oxide and its nanocomposites was analyzed by using field emission scanning electron microscopy (JEOL, JSM-7610F) and transmission electron microscopy (JEOL, JEM-2100F, 200KV TEM).The analysis system was equipped with high-energy laser diodes. Melting points were determined in open capillaries with a Galen-Kamp melting point apparatus and are not corrected. The thermal degradation pattern of the synthesized nanocomposite was determined by thermogravimetric analysis (TGA) using a thermal analyzer TA-SDT Q-600. The magnetic properties of the prepared catalyst were investigated by using a VSM with an applied field between -8,000 and 8,000 Oe at room temperature (MDKF, Iran). ICPOES spectrometer (Thermo Scientific, IRIS Intrepid II, USA) were used for determination the loading amounts of Cu on the surface of prepared nanocomposites.

Experimental

Synthesis of Fe_3O_4 nanoparticles, Fe_3O_4-CuO and CNT/Fe_3O_4-CuO nanocomposites, their characterizations and full characterization of the catalyst rGO/Fe_3O_4-CuO have been reported in our recent published article.[1]

Characterization of rGO/Fe_3O_4-CuO: The FT-IR spectra of GO, rGO, rGO/Fe_3O_4 and rGO/Fe_3O_4-CuO are shown in Figure 1.

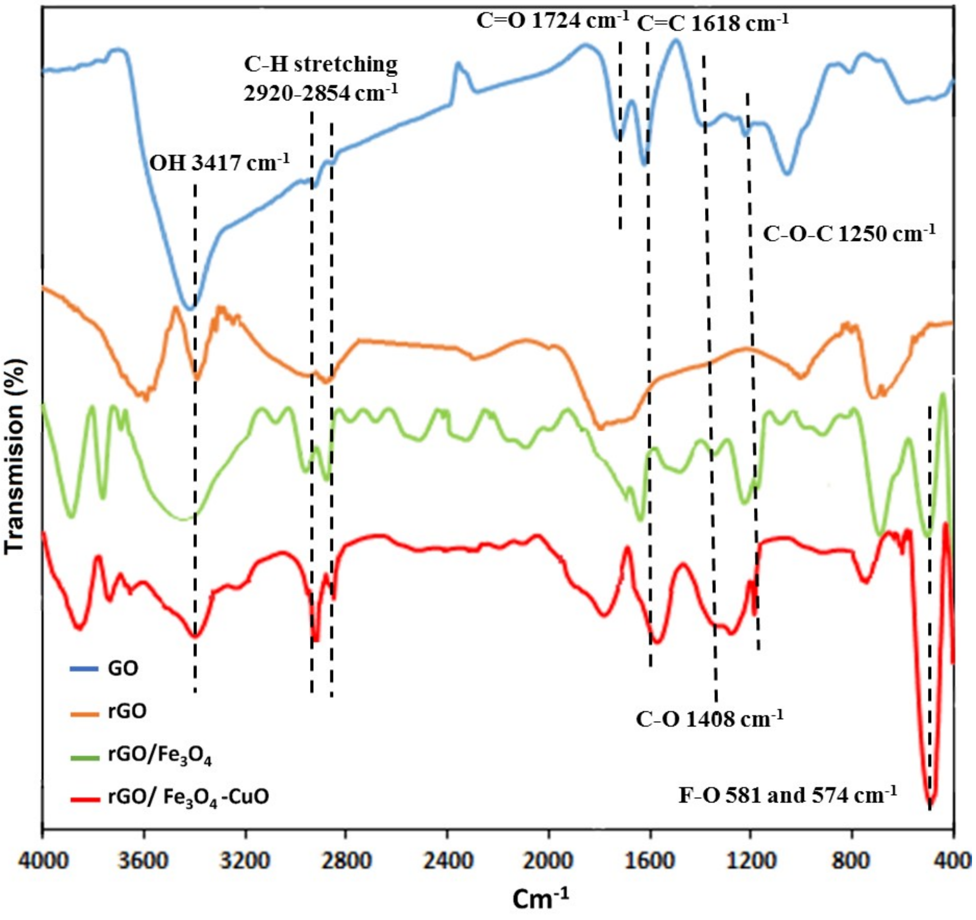

Figure 1: FT-IR spectra of GO, rGO, rGO/Fe_3O_4 and rGO/Fe_3O_4-CuO

The FT-IR spectrum of GO contained peaks assignable to the following absorption modes: -OH stretching (3417 cm^{-1}), C=O stretching (1724 cm^{-1}), aromatic C=C (1618 cm^{-1}), carboxy C-O (1408 cm^{-1}), C-O-C (1250 cm^{-1}), C-O (1049 cm^{-1}). The IR spectrum also showed the reduction of GO to rGO by the reduction of the intensity of oxygen containing functional groups. The FTIR spectrum of rGO/Fe_3O_4 composite showed the new and intense peak at 581 cm^{-1} which is corresponded to the vibration of Fe-O bonds in the crystalline lattice of Fe_3O_4. Moreover, the peak at 1724 cm^{-1} (C=O) diminished due to the formation of carboxylate groups (-COO^-) after coating with Fe_3O_4.[2] The peak position of -Fe-O- stretching vibration in GO/Fe_3O_4 was slightly shifted (to 574 cm^{-1}) after adsorption of copper on the GO surfaces. The characteristic C=C band was also shifted to 1610 cm^{-1}. These shifts in peak positions show the succesful formation of the metal-ligand bond.

Figure 2 shows the X-ray diffraction (XRD) profiles of GO (A), rGO (B), rGO/Fe_3O_4 (C) and rGO/Fe_3O_4-CuO (D). As shown in Fig. 2, the GO displays a strong diffraction peak at 2θ = 11.7° indicating an interlayer spacing of 0.76 nm. This diffraction peak is assigned to the (001) reflection of stacked GO.[3] In the XRD pattern of rGO, the major peak is observed at about 23.9°. This gives an interlayer spacing of approximately 0.37 nm.

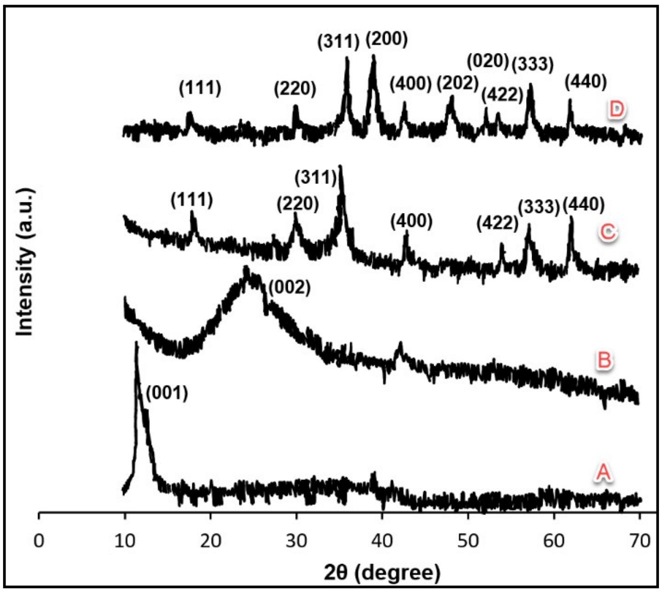

Figure 2: XRD pattern of (A) GO, (B) rGO, (C) rGO/Fe_3O_4 and (D) rGO/Fe_3O_4-CuO

Magnetic rGO shows the characteristic peaks for the spinal Fe_3O_4 phase at 2θ = 18.7° (111), 30.5° (220), 35.8° (311), 43.4° (400), 54.1° (422), 57.9° (333) and 63.1° (440) (JCPDS No. 75-0033), in addition to a broad peak positioned around 24° which is attributed to rGO.[4] Catalyst rGO/Fe_3O_4-CuO shows additional peaks due to CuO at 2θ = 38.6°, 48.6°, and 53.3°, corresponding to the (200), (202), and (020) planes of copper oxide (JCPDS No. 80-1268).[5]

The magnetic properties of rGO/Fe_3O_4-CuO, was investigated by room temperature vibrating sample magnetometer (VSM) and the maximum saturation magnetization (*Ms*) value of the catalyst was estimated (Figure 3).

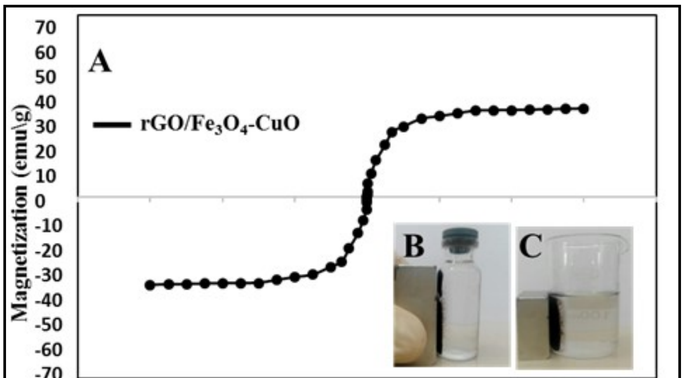

Figure 3. Hysteresis curve of rGO/Fe_3O_4-CuO at 300 K (A), Magnetic behavior of rGO/Fe_3O_4 (B) and rGO/Fe_3O_4-CuO (C).

The obtained results showed that magnetic hysteresis loop is S-like with the maximum saturation magnetization (Ms) of 34.6 emu/g. This value shows that the prepared nanocomposite is superparamagnetic. It can be also observed that the Ms of the composite is smaller than the reported value of bulk Fe_3O_4 which is due to the relatively low loading amount of the Fe_3O_4 NPs in the composite.

The thermal behavior of the GO, rGO, rGO/Fe_3O_4 and rGO/Fe_3O_4-CuO hybrid were investigated by TG analysis under nitrogen atmosphere and the related curves are shown in Figure 4. GO shows mass losses at two temperature ranges: initial weight loss of GO from temperature to 150 °C could be primarily due to evaporation of water molecules held in the samples. The second one occurs, at approximately 200-260 °C, due to the removal of some of the oxygen-containing functional groups.[6] Finally, the gradual mass loss above 260 °C might have resulted from the further removal of functional groups.

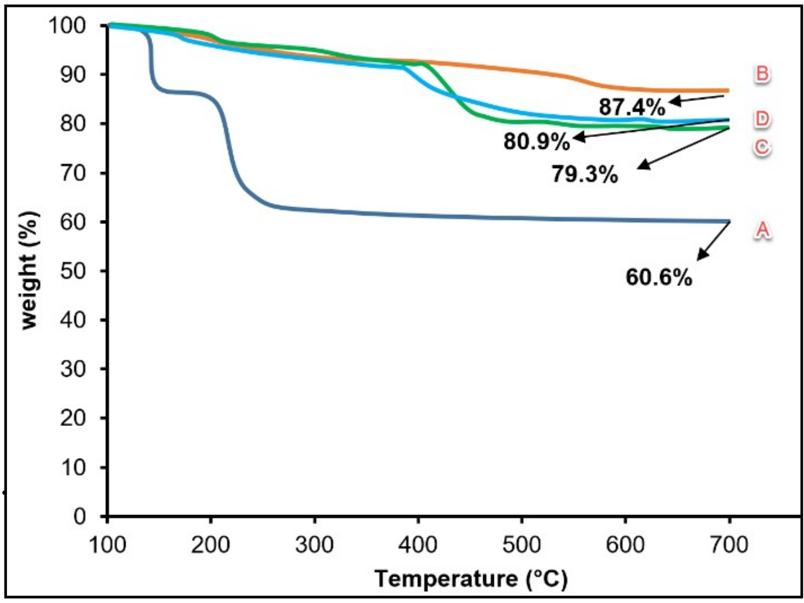

Figure 4. $_4$-CuO.

The weight loss 150 °C, which is much smaller than that for GO, could be attributed to adsorbed water too. In the range of 200-260 °C, rGO, rGO/Fe_3O_4 and rGO/Fe_3O_4-CuO hybrid lose only 2-3% of their weight. In the case of rGO/Fe_3O_4, the main weight loss (12%) occurs at 400-500 °C, due to the bulk pyrolysis of carbon skeleton.[7] For the rGO/Fe_3O_4-CuO hybrid, a weight loss of 10% occurred from ~400-500 °C, which is due to the further carbonization of the graphene backbone.[8]

The surface morphology and structural features of rGO/Fe_3O_4-CuO were illustrated by Transmission electron microscopy (TEM) and scanning electron microscopy (FESEM). TEM (Fig. 5A), FESEM (Fig. 5B) and EDS mapping (Fig. 5C) images of the catalyst show that the magnetite and copper nanoparticles are homogeneously deposited on rGO in the entire surface of rGO.

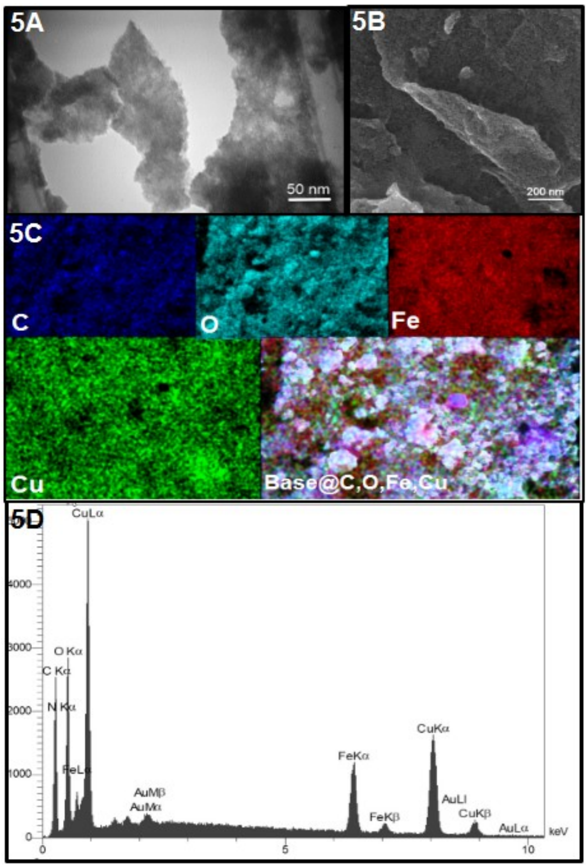

Figure 5. TEM image of rGO/Fe_3O_4-CuO (A); FESEM image of rGO/Fe_3O_4-CuO (B); EDX elemental mapping images of the surface of rGO/Fe_3O_4-CuO (C) and EDX analysis of rGO/Fe_3O_4-CuO (D).

These changes confirmed that the true chemical modification has been achieved. The energy-dispersive X-ray analysis (EDX) analysis was also applied to determine the elemental composition and show the presence of Fe and Cu elements in the rGO/Fe_3O_4-CuO hybrid. The EDX spectrum shows intense peaks for Fe and Cu along with carbon and oxygen peaks. This suggests the grafting of Fe_3O_4-CuO on the surface of rGO.

The surface area of this material was determined via the BET method, and the N_2 adsorption-desorption isotherms are shown in Fig. 6. Analysis of the data using Brunauer-Emmett-Teller (BET) method gave a specific surface area (S_{BET}) of 202 m^2 g^{-1} for fresh hybrid material.

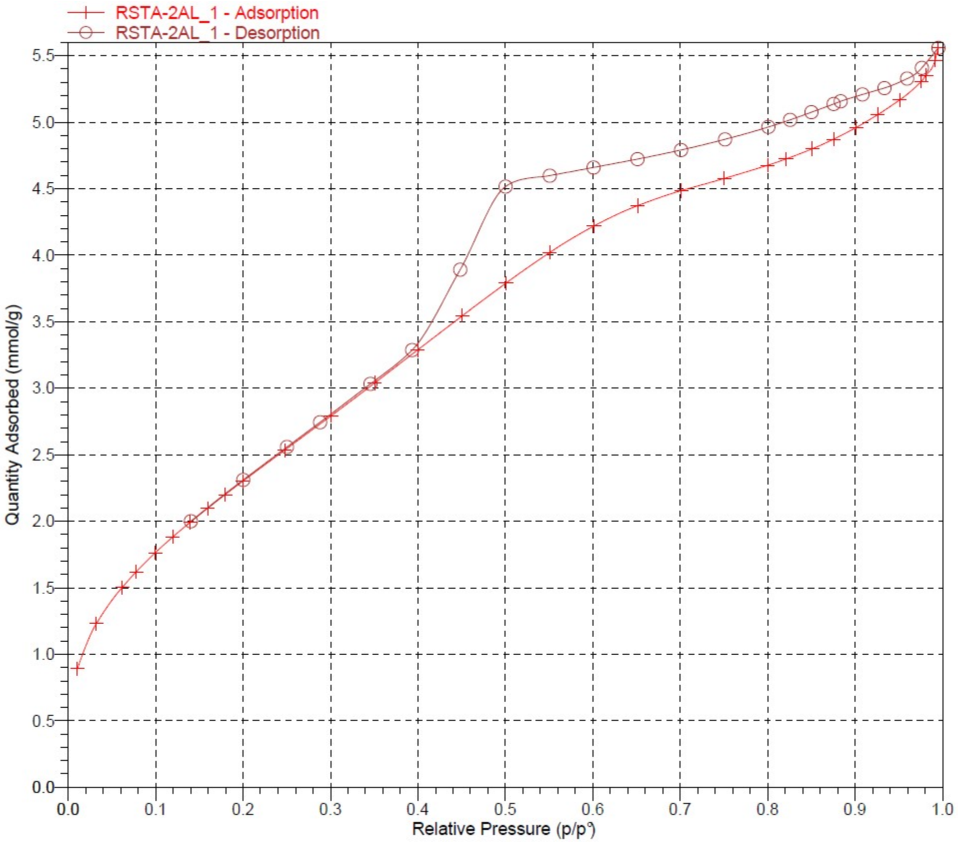

Figure 6: Nitrogen adsorption-desorption isotherm of the rGO/Fe_3O_4-CuO

Spectral data of reported benzyl benzoate derivatives

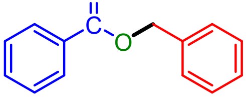

Benzyl benzoate (3a)[9]: Yellow liquid; ^{1}H-NMR (250 MHz, $CDCl_3$): δ (ppm) = 7.94-7.98 (m, 2H), 7.23-7.41 (m, 8H), 5.25 (s, 2H); ^{13}C-NMR (62.5 MHz, $CDCl_3$): δ (ppm) = 166.5, 136.2, 133.0, 130.1, 129.7, 128.6, 128.5, 128.3, 128.2, 66.8.

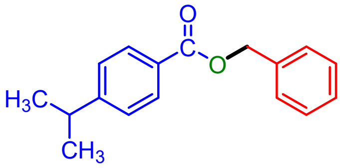

Benzyl 4-isopropylbenzoate (3b)[10]: Yellow liquid; ^{1}H-NMR (250 MHz, $CDCl_3$): *δ* (ppm) = 7.92 (d, *J* = 7.5 Hz, 2H), 7.28-7.38 (m, 3H), 7.15-7.23 (m, 4H), 5.28 (s, 2H), 2.79-2.93 (m, 1H), 1.18 (d, *J* = 5.0 Hz, 6H); ^{13}C-NMR (62.5 MHz, $CDCl_3$): *δ* (ppm) = 166.9, 147.9, 131.9, 129.3, 128.9, 127.5, 127.3, 125.6, 125.4, 65.6, 32.9, 23.0, 22.8.

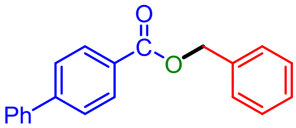

Benzyl 4-phenylbenzoate (3c)[11]: Colorless liquid; ^{1}H-NMR (250 MHz, $CDCl_3$): *δ* (ppm) = 8.08 (d, *J* = 7.5 Hz, 2H),7.54-7.61 (m, 4H), 7.32-7.44 (m, 8H), 5.32 (s, 2H);^{13}C-NMR (62.5 MHz, $CDCl_3$): *δ* (ppm) = 167.3, 143.0, 142.2, 137.1, 129.9, 129.3, 128.6, 128.0, 127.4,127.2, 127.1, 126.3, 126.2, 65.2.

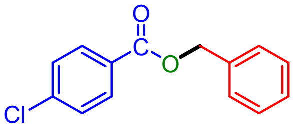

Benzyl 4-chlorobenzoate (3d)[9]: Yellow oil; ^{1}H-NMR (400 MHz, $CDCl_3$): *δ* (ppm) = 8.05 (d, *J* = 7.5 Hz, 2H); 7.56-7.58 (m, 2H), 7.41-7.49 (m, 5H), 5.39 (s, 2H); ^{13}C NMR (100 MHz, $CDCl_3$): δ (ppm) = 167.8, 132.5, 131.1, 130.9, 129.5, 128.8, 128.8, 128.7, 128.3, 127.8, 67.0.

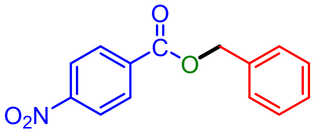

Benzyl 4-nitrobenzoate (3e)[9]: Pale yellow solid; m.p. = 83-84 °C. ^{1}H-NMR (250 MHz, $CDCl_3$): *δ* (ppm) = 8.13-8.21 (m, 4H), 7.17-7.40 (m, 5H), 5.30 (s, 2H); ^{13}C-NMR (62.5 MHz, $CDCl_3$): *δ* (ppm) = 164.6, 150.5, 135.4, 135.2, 130.8, 128.7, 128.6, 128.5, 123.5, 67.7.

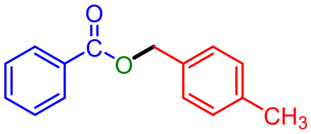

Benzyl 4-methylbenzoate (3f)[12]: Yellow oil; ^{1}H NMR (250 MHz, $CDCl_3$): *δ* (ppm) = 7.97-8.04 (m, 2H), 7.29-7.39 (m, 7H), 5.25 (s, 2H), 2.33 (s, 3H); ^{13}C NMR (62.5 MHz, $CDCl_3$): *δ* (ppm) = 165.1, 136.2, 132.0, 131.9, 128.7, 128.1, 127.5, 127.3, 127.2, 65.5, 28.3.

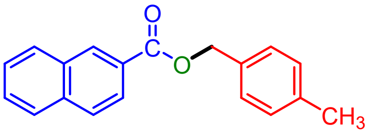

4-Methylbenzyl 2-naphthoate (3g): Yellow oil; ^{1}H-NMR (250 MHz, $CDCl_3$): *δ* (ppm) = 8.86 (d, *J* = 7.5 Hz, 1H), 8.10-8.14 (m, 1H), 7.91 (dd, *J* = 7.5, 2.5 Hz, 1H), 7.77 (d, *J* = 7.5 Hz, 1H), 7.29-7.55 (m, 5H), 7.10-7.14 (m, 2H), 5.22 (s, 2H), 2.30 (s, 3H); ^{13}C-NMR (62.5 MHz, $CDCl_3$): *δ* (ppm) = 167.3, 138.1, 133.8, 133.4, 133.1, 131.4, 130.4, 129.3, 128.5, 128.5, 127.8, 127.0, 126.2, 125.8, 124.5, 66.8, 21.2.

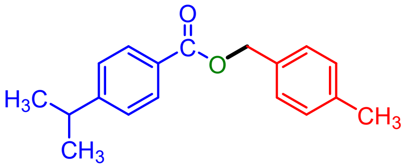

4-Methylbenzyl 4-isopropylbenzoate (3h): Colorless oil; ^{1}H NMR (250 MHz, $CDCl_3$): *δ* (ppm) = 7.89-7.93 (m, 2H), 7.11-7.27 (m, 6H), 5.23 (s, 2H), 2.78-2.92 (m, 1H), 2.31 (s, 3H), 1.18 (d, *J* = 2.5 Hz, 3H), 1.15 (d, *J* = 2.5 Hz, 3H); ^{13}C NMR (62.5 MHz, $CDCl_3$): *δ* (ppm) = 166.5, 153.0, 138.3, 133.0, 129.7, 129.0, 128.3, 126.4, 126.3, 67.3, 33.9, 24.0, 21.7.

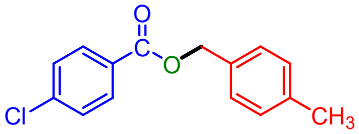

4-Methylbenzyl 4-chlorobenzoate (3i)[13]: White solid; m.p. = 54-56 °C. ^{1}H-NMR (250 MHz, $CDCl_3$): *δ* (ppm) = 7.86-7.94 (m, 2H), 7.23-7.33 (m, 4H), 7.09-7.13 (m, 2H), 5.22 (s, 2H), 2.31 (s, 3H); ^{13}C-NMR (62.5 MHz, $CDCl_3$): *δ* (ppm) = 164.7, 138.3, 137.2, 131.8, 130.1, 128.8, 128.2, 127.8, 127.3, 65.6, 20.6.

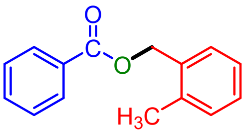

2-Methylbenzyl benzoate (3j)[14]: Colorless liquid; ^{1}H-NMR (250 MHz, $CDCl_3$): δ (ppm) = 7.97-8.02 (m, 2H), 7.44-7.45 (m, 1H), 7.31-7.38 (m, 3H), 7.13-7.17 (m, 3H), 5.27 (s, 2H), 2.35 (s, 3H); ^{13}C-NMR (62.5 MHz, $CDCl_3$): δ (ppm) = 166.9, 140.3, 139.2, 132.8, 130.4, 129.7, 129.2, 128.6, 128.2, 126.1, 64.9, 29.3.

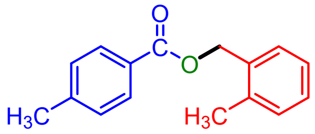

2-Methylbenzyl 4-methylbenzoate (3k)[15]: Yellow oil; ^{1}H-NMR (250 MHz, $CDCl_3$): δ (ppm) = 7.89 (d, J = 7.5 Hz, 2H), 7.33-7.37 (m, 1H), 7.14-7.18 (m, 5H), 5.29 (s, 2H), 2.34 (s, 6H); ^{13}C-NMR (62.5 MHz, $CDCl_3$): δ (ppm) = 166.6, 143.7, 137.1, 134.1, 130.4, 129.7, 129.2, 129.1, 128.5, 127.4, 126.0, 65.1, 21.7, 19.0.

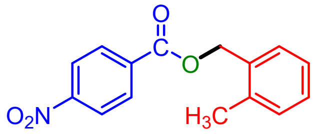

2-Methylbenzyl 4-nitrobenzoate (3l)[16]: Pale yellow solid; m.p.= 103-105 °C. ^{1}H-NMR (250 MHz, $CDCl_3$): δ (ppm) = 8.10-8.20 (m, 4H), 7.31-7.35 (m, 1H), 7.12-7.24 (m, 3H), 5.30 (s, 2H), 2.29 (s, 3H); ^{13}C-NMR (62.5 MHz, $CDCl_3$): δ (ppm) = 164.5, 150.7, 137.5, 135.3, 133.3, 131.1, 130.4, 129.7, 129.2, 126.0, 123.8, 65.7, 19.2.

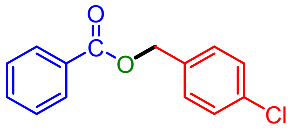

4-Chlorobenzyl benzoate (3m)[17]: White solid; m.p.= 58-60 °C. ^{1}H-NMR (250 MHz, $CDCl_3$): δ (ppm) = 7.95-8.00 (m, 2H), 7.27-7.47 (m, 7H), 5.23 (s, 2H); ^{13}C-NMR (62.5 MHz, $CDCl_3$): δ (ppm) = 166.5, 134.5, 134.1, 133.3, 130.0, 129.9, 129.5, 129.0, 128.6, 66.2.

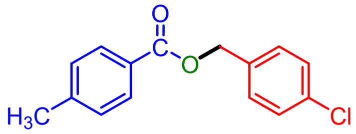

4-Chlorobenzyl 4-methylbenzoate (3n)[17]: Yellow liquid; ^{1}H-NMR (250 MHz, $CDCl_3$): δ (ppm) = 7.85-7-89 (m, 2H), 7.12-7.31 (m, 6H), 5.22 (s, 2H), 2.27 (s, 3H); ^{13}C-NMR (62.5 MHz, $CDCl_3$): δ (ppm) = 166.5, 144.0, 134.8, 134.1, 129.8, 129.4, 129.0, 128.9, 127.2, 65.5, 21.6.

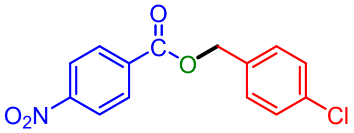

4-Chlorobenzyl 4-nitrobenzoate (3o)[18]: Yellow solid, mp = 113-115 °C; ^{1}H-NMR (250 MHz, $CDCl_3$): δ (ppm) = 8.12-8.22 (m, 4H), 7.26-7.34 (m, 4H), 5.28 (s, 2H); ^{13}C-NMR (62.5 MHz, $CDCl_3$): δ (ppm) = 164.5, 150.6, 135.3, 134.6, 133.8, 130.8, 129.9, 129.0, 123.6, 66.8.

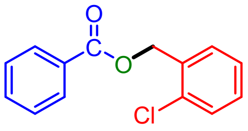

2-Chlorobenzyl benzoate (3p)[19]: Colorless oil; ^{1}H-NMR (250 MHz, $CDCl_3$): δ (ppm) = 8.01-8.05 (m, 2H), 7.32-7.54 (m, 5H), 7.20-7.26 (m, 2H), 5.41 (s, 2H); ^{13}C-NMR (62.5 MHz, $CDCl_3$): δ (ppm) = 166.3, 135.0, 133.8, 133.2, 130.0, 129.8, 129.8, 129.7, 129.6, 128.5, 126.9, 64.1.

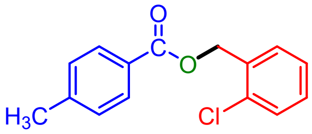

2-Chlorobenzyl 4-methylbenzoate (3q)[17]: Yellow oil; ^{1}H-NMR (250 MHz, $CDCl_3$): δ (ppm) = 7.92 (d, J = 7.5 Hz, 2H), 7.32-7.45 (m, 2H), 7.15-7.24 (m,4H), 5.36 (s, 2H), 2.37 (s, 3H); ^{13}C-NMR (62.5 MHz, $CDCl_3$): δ (ppm) = 166.4, 143.6, 134.4, 134.1, 129.9, 129.6, 129.5, 129.4, 129.2, 127.3, 127.0, 64.1, 22.0.

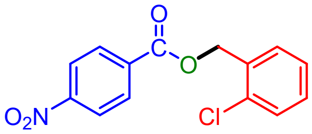

2-Chlorobenzyl 4-nitrobenzoate (3r)[20]: Yellow solid; mp = 88-90 °C; ^{1}H-NMR (250 MHz, $CDCl_3$): δ (ppm) = 8.13-8.21 (m, 4H), 7.32-7.43 (m, 2H), 7.21-7.25 (m, 2H), 5.42 (s, 2H); ^{13}C-NMR (62.5 MHz, $CDCl_3$): δ (ppm) = 164.2, 150.9, 135.2, 133.9, 133.0, 130.7, 130.4, 130.1, 129.6, 127.1, 123.7, 64.9.

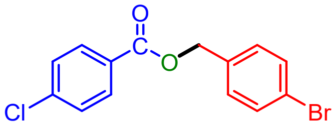

4-Bromobenzyl 4-chlorobenzoate (3s)[21]: Colorless oil; ^{1}H-NMR (250 MHz, $CDCl_3$): δ (ppm) = 7.90-7.94 (m, 2H), 7.42-7.48 (m, 2H), 7.32-7.37 (m, 2H), 7.23-7.27 (m, 2H), 5.21 (s, 2H); ^{13}C-NMR (62.5 MHz, $CDCl_3$): δ (ppm) = 166.0, 139.2, 134.7, 131.7, 131.0, 130.0, 128.7, 128.2, 124.0, 65.9.

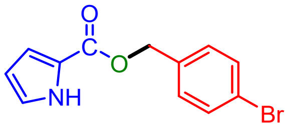

4-Bromobenzyl 1H-pyrrole-2-carboxylate (3t): Yellow oil; ^{1}H-NMR (250 MHz, $CDCl_3$): δ (ppm) = 7.84 (d, J = 7.5 Hz, 2H), 7.64 (s, 1H), 7.43-7.53 (m, 4H), 7.26-7.27 (m, 1H), 5.23 (s, 2H); ^{13}C NMR (62.5 MHz, $CDCl_3$): δ (ppm) = 163.3, 135.7, 132.6, 131.2, 122.4, 121.7, 121.6, 112.7, 110.7.

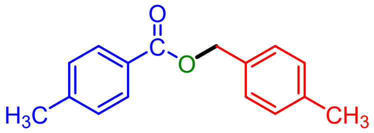

4-Methylbenzyl 4-methylbenzoate (3u)[22]: Pale yellow oil; ^{1}H-NMR (400 MHz, $CDCl_3$): δ (ppm) = 8.00 (d, J = 5.0 Hz, 2H), 7.39 (d, J = 5.0 Hz, 2H), 7.23-7.28 (m, 4H), 5.35 (s, 2H), 2.44 (s, 3H), 2.41 (s, 3H); ^{13}C NMR (100 MHz, $CDCl_3$): δ (ppm) = 166.6, 143.7, 138.1, 133.2, 129.8, 129.3, 129.1, 128.4, 127.5, 66.5, 21.7, 21.3.

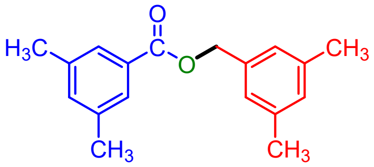

3,5-Dimethylbenzyl 3,5-dimethylbenzoate (3v)[23]: Colorless oil; ^{1}H-NMR (250 MHz, $CDCl_3$): δ (ppm) = 7.69 (2H, s), 7.18 (1H, s), 7.06 (2H, s), 6.98 (1H, s), 5.27 (2H, s), 2.33, 2.35 (12H, s); ^{13}C NMR (62.5 MHz, $CDCl_3$): δ (ppm) = 166.9, 138.2, 138.0, 136.0, 134.6, 129.9, 129.6, 127.4, 126.2, 66.7, 21.3, 21.2.

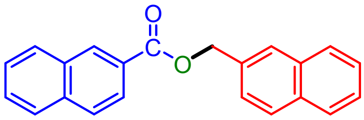

Naphthalen-2-ylmethyl 2-naphthoate (3w)[24]: White solid; mp = 98-100 °C. ^{1}H-NMR (400 MHz, $CDCl_3$): δ (ppm) = 8.71 (s, 1H), 8.16 (d, J = 5.0 Hz, 1H), 7.92-8.00 (m, 7H), 7.54-7.66 (m, 5H), 5.63 (s, 2H); ^{13}C NMR (100 MHz, $CDCl_3$): δ (ppm) = 166.7, 135.6, 133.5, 133.3, 133.2, 132.5, 131.3, 129.4, 128.5, 128.3, 128.2, 128.1, 127.8, 127.8, 127.5, 126.7, 126.4, 126.3, 126.0, 125.3, 67.1.

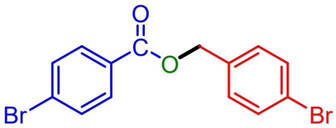

4-Bromobenzyl 4-bromobenzoate (3x)[25]: White solid; mp = 103-105 °C. ^{1}H-NMR (250 MHz, $CDCl_3$): δ (ppm) = 7.29-7.93 (m, 8H), 5.29 (s, 2H); ^{13}C NMR (62.5 MHz, $CDCl_3$): δ (ppm) = 165.6, 134.8, 131.8, 131.8, 131.2, 130.0, 128.8, 128.4, 122.5, 66.2.

References

1. Rousta, M; Khalili, D; Khalafi-Nezhad, A; Ebrahimi, E. New J. Chem. 2021, 45, 20007-20020.
2. Xiong, X; Chen, H; Tang, Z; Jiang, Y. *RSC Adv.*, 2014, 4, 9830-9837.
3. Fan, Z; Wang, K; Wei, T; Yan, J; Song, L; Shao, B. *Carbon*, 2010, 48, 1686-1689.
4. Chandra, V; Park, J; Chun, Y; Lee, J. W; Hwang, I.-C; Kim, K. S. *ACS Nano*, 2010, 4, 3979-3986.
5. Raul, P. K; Senapati, S; Sahoo, A. K; Umlong, I. M; Devi, R. R; Thakur, A. J; Veer, V. *RSC Adv.*, 2014, 4, 40580-40587.
6. Li, F; Guo, Y; Liu, Y; Yan, J; Wang, W; Gao, J. *Carbon*, 2014, 67, 617-626.
7. Boruah, P. K; Borah, D. J; Handique, J; Sharma, P; Sengupta, P; Das, M. R. *J. Environ. Chem. Eng.*, 2015, **3**, 1974-1985.
8. Liu, Y; Zhou, J; Zhang, X; Liu, Z; Wan, X; Tian, J; Wang, T; Chen, Y. *Carbon*, 2009, **47**, 3113-3121.
9. Huang, H.; Yong Kang, J. *Org. Lett.* 2017, 19, 3, 544-547.
10. Lai, M; Qi, X; Wu, X-F. Eur. *J. Org. Chem.,* 2019, 2019, 3776- 3778.

11. Rout, S. K; Guin, S; Ghara, Krishna K; Banerjee, A; Patel, B. K. *Org. Lett.* 2012, 14, 3982-3985.
12. Yasuhide, Y; Yuho, T; Masami, S. *Bull. Chem. Soc. Jpn.* 1972, 45, 1198-1205.
13. Kwon, Y. D; La, M. T; Kim, H. K. *New J. Chem.*, 2018, 42, 10833-10841.
14. Subaramanian, M; Ramar, P. M.; Rana, J; Gupta, V. K; Balaraman, E. *Chem. Commun.* 2020, 56, 8143-8146.
15. Iranpoor, N; Firoozabadi, H; Khalili, D. *Org. Biomol. Chem.* 2010, ***8***, 4436-4443.
16. Mozingo, R; Folkers K. *J. Am. Chem. Soc.* 1948, 70, 1, 229-231.
17. Bahrami, K; Khodaei, M. M.; Targhan, H; Sheikh Arabi, M. *Tetrahedron Lett.* 2013, 54, 5064-5068.
18. Phungpis, H; Hahnvajanawong, V. *Asian. J. Chem.* 2021, 33, 2671-2674.
19. Lu, B; Zhu, F; Sun, H-M; Shen, Q. *Org. Lett.* 2017, 19, 5, 1132-1135.
20. Rosenmund; Z. *Chem. Ber*, 1921, 54, 2036.
21. Shen, H; Lu, X; Jiang, K-Z; Yang, K-F; Lu, Y; Zheng, Z-J; Lai, G-Q; Xu, L-W. *Tetrahedron*, 2012, 68, 8916-8923.
22. Jiang, X; Zhang, J; Zhao, D; Li, Y. *Chem. Commun*., 2019, 55, 2797-2800.
23. Ogoshi, S; Hoshimoto, Y; Ohashi, M. *Chem. Commun.,* 2010, 46, 3354-3356.
24. Grushin, V. V.; Alper, H. *J. Org. Chem.,* 1991, 56, 5159-5161.
25. Simon, M-O; Darses, S. *Adv. Synth. Catal.,* 2010, 352, 305-308.

Copy of ^{1}H-NMR and ^{13}C-NMR of products

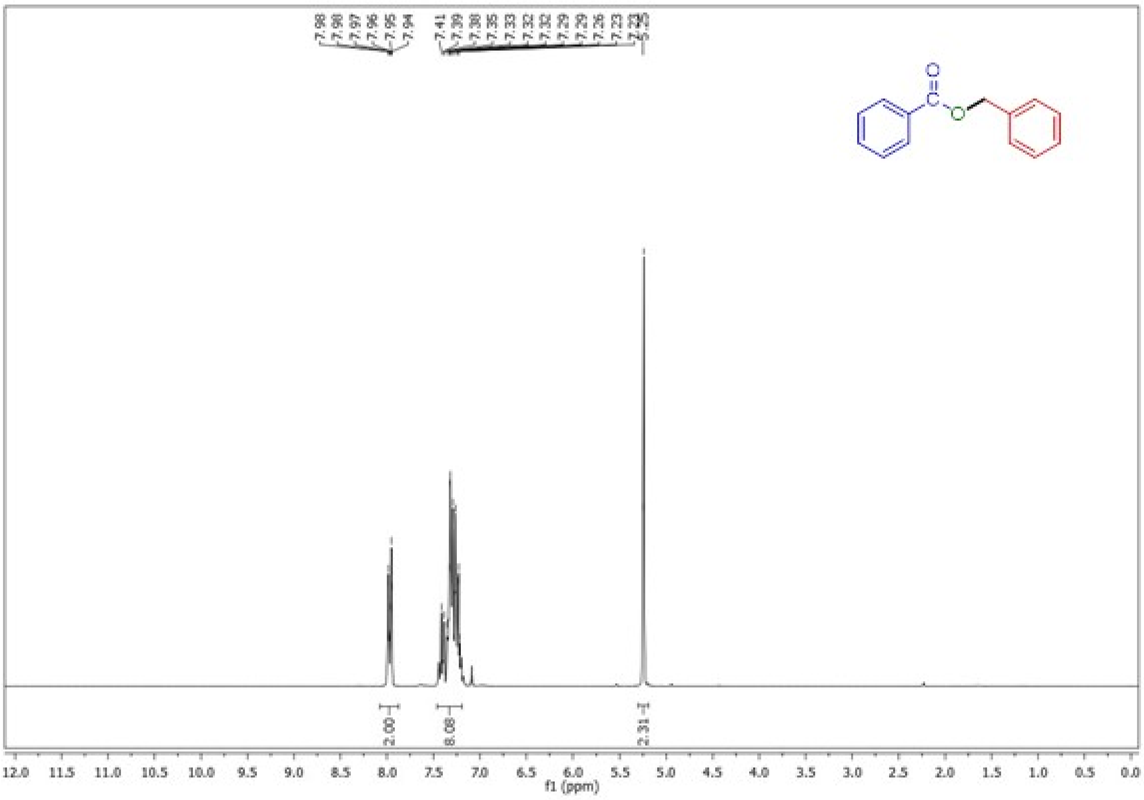

^{1}H-NMR of **3a**

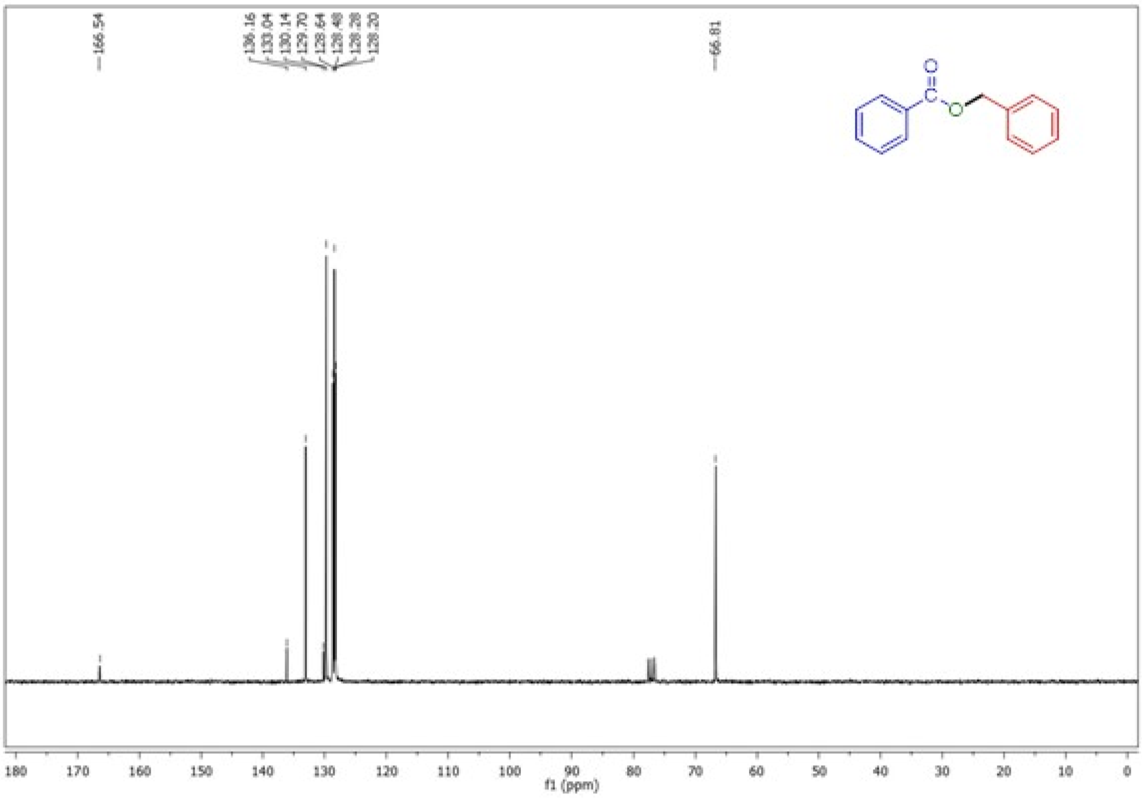

^{13}C-NMR of **3a**

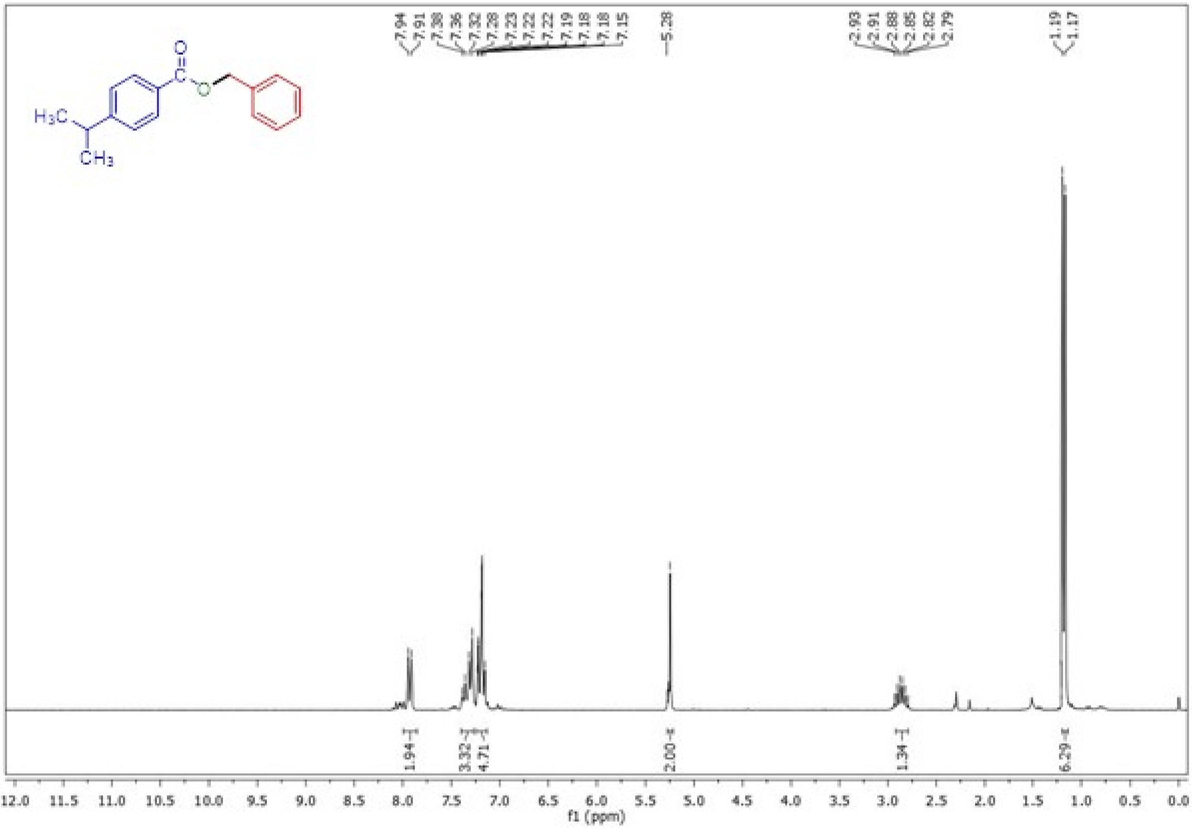

^{1}H-NMR of **3b**

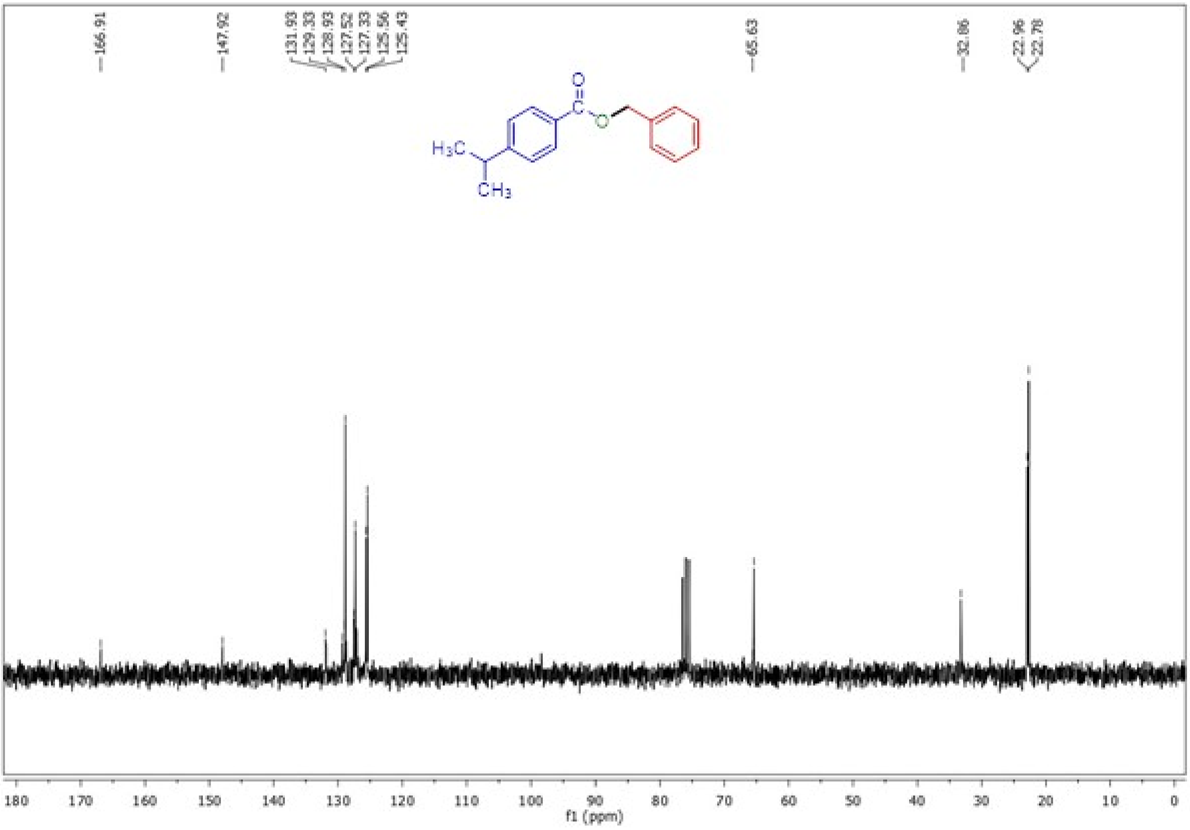

^{13}C-NMR of **3b**

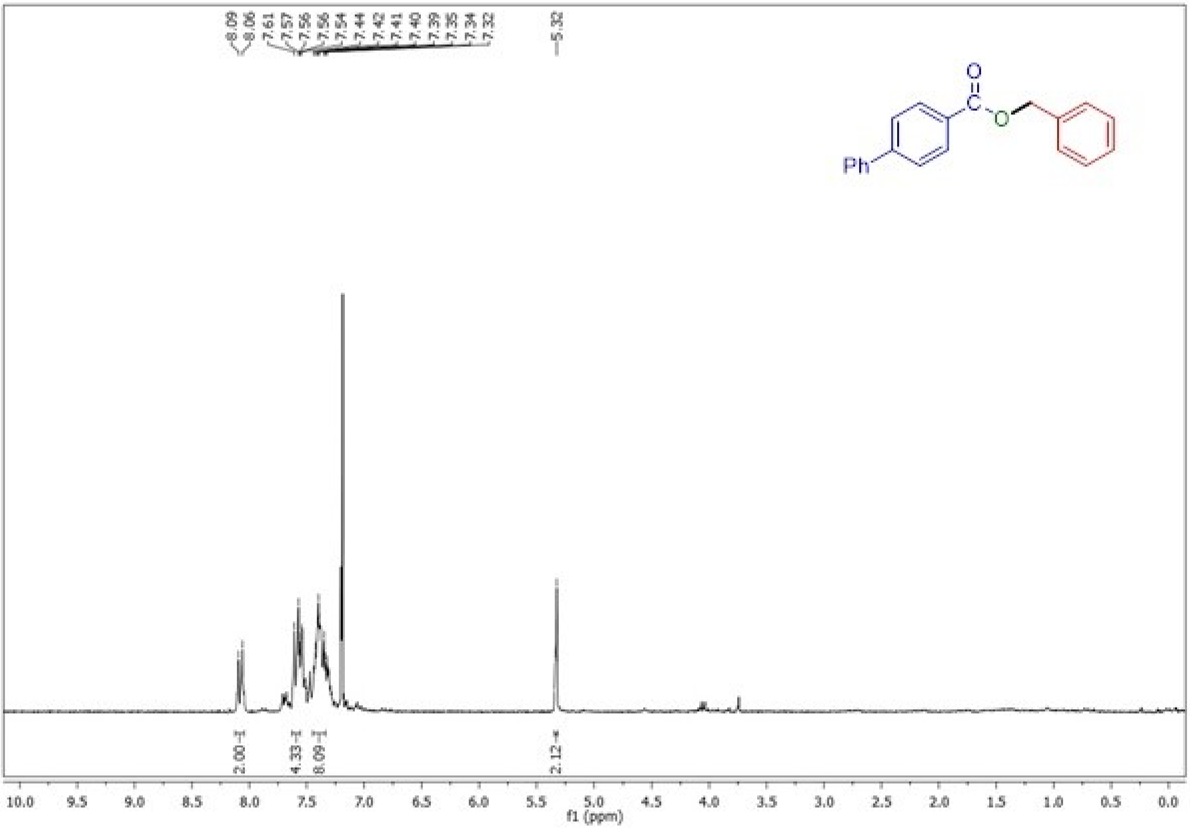

^{1}H-NMR of **3c**

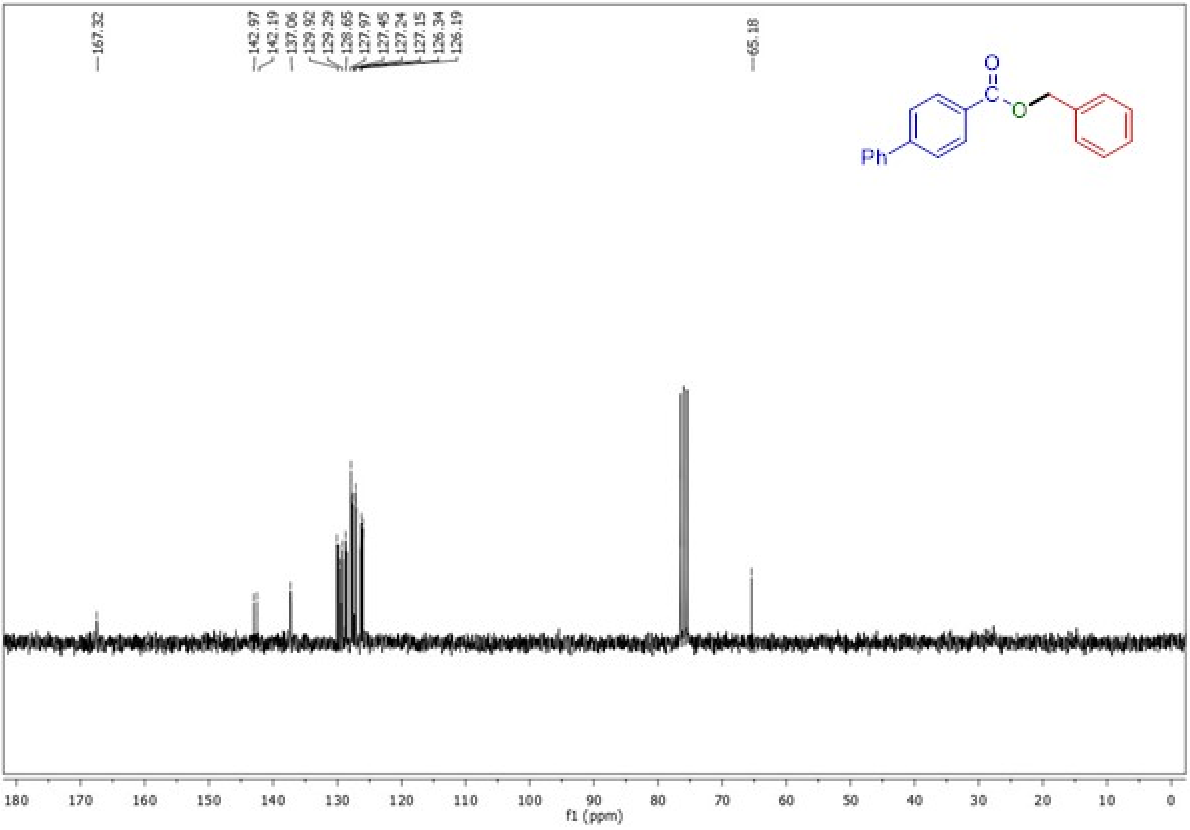

^{13}C-NMR of **3c**

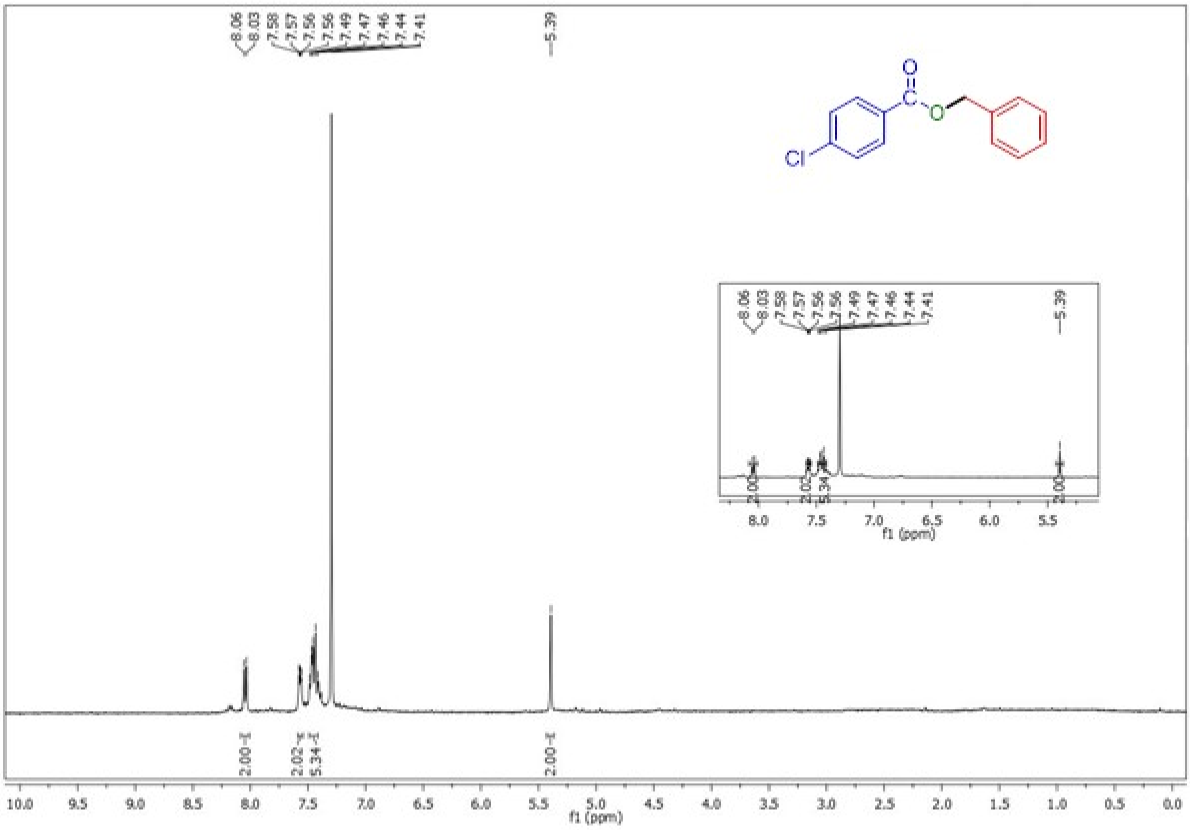

^{1}H-NMR of **3d**

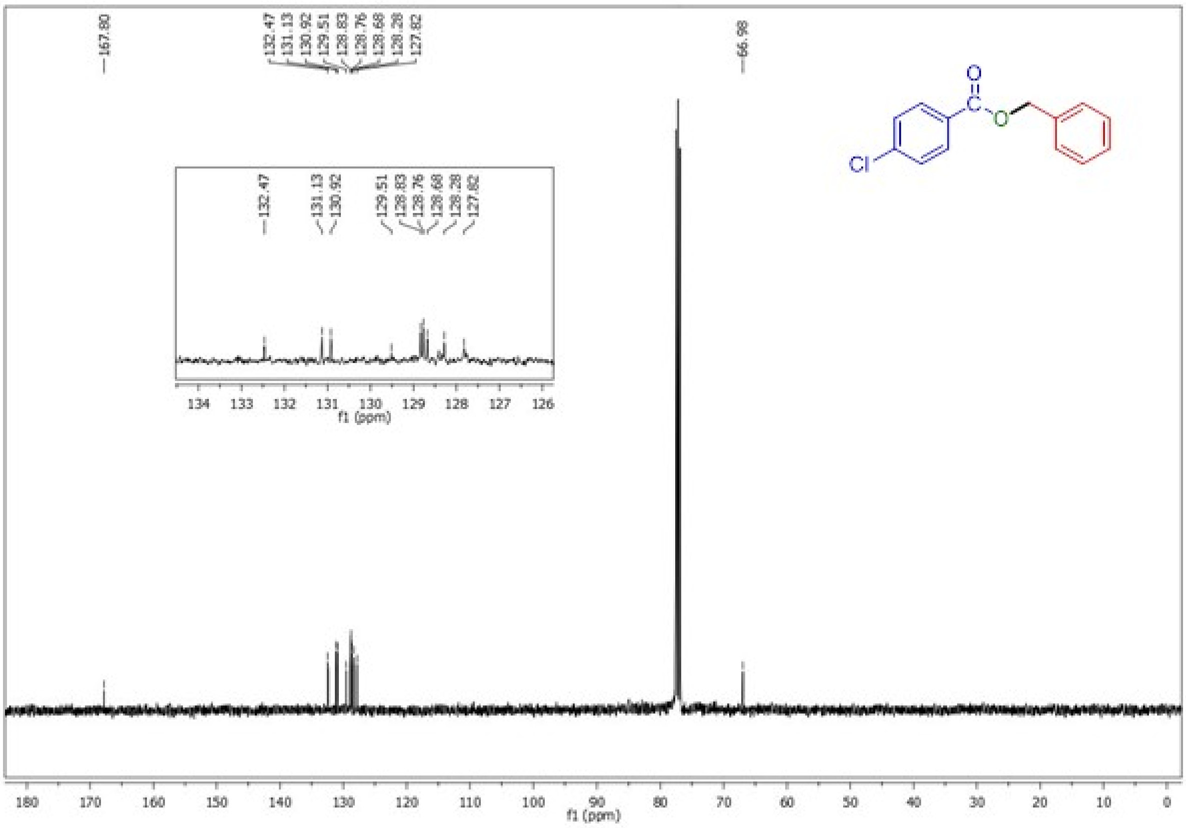

^{13}C-NMR of **3d**

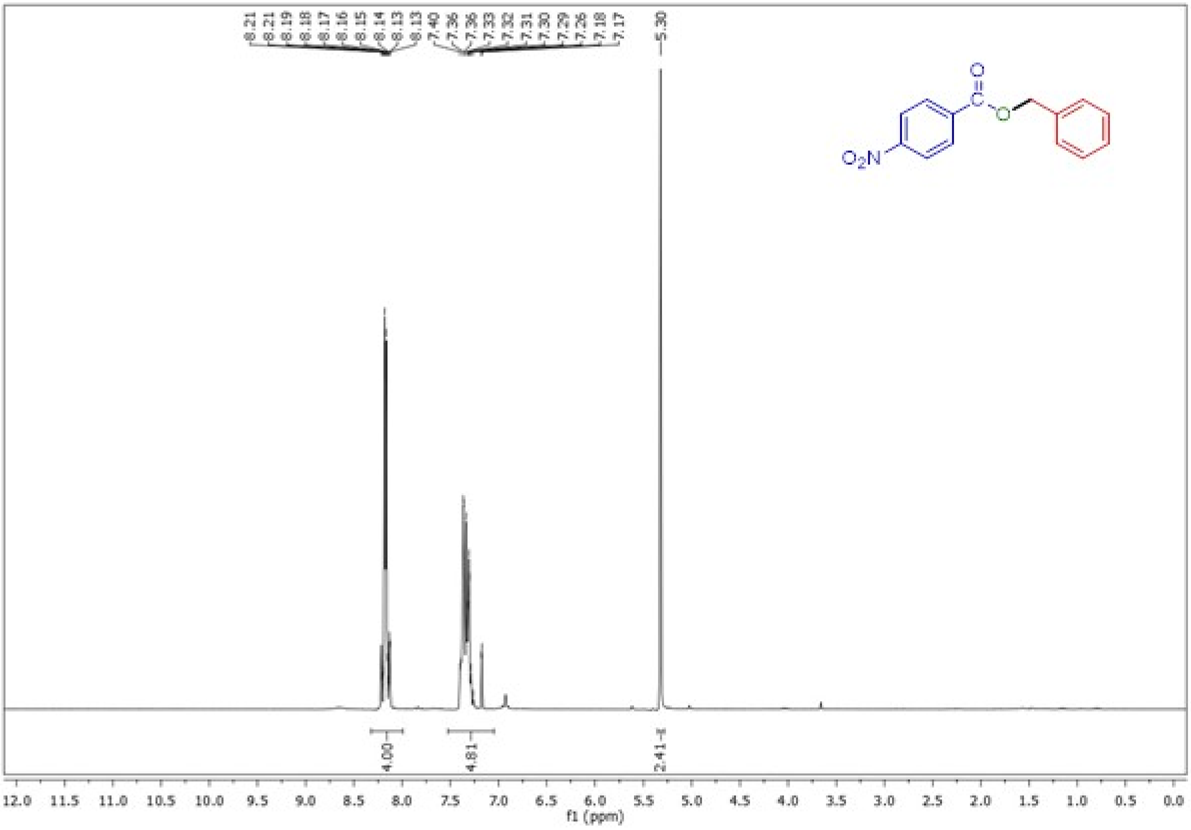

^{1}H-NMR of **3e**

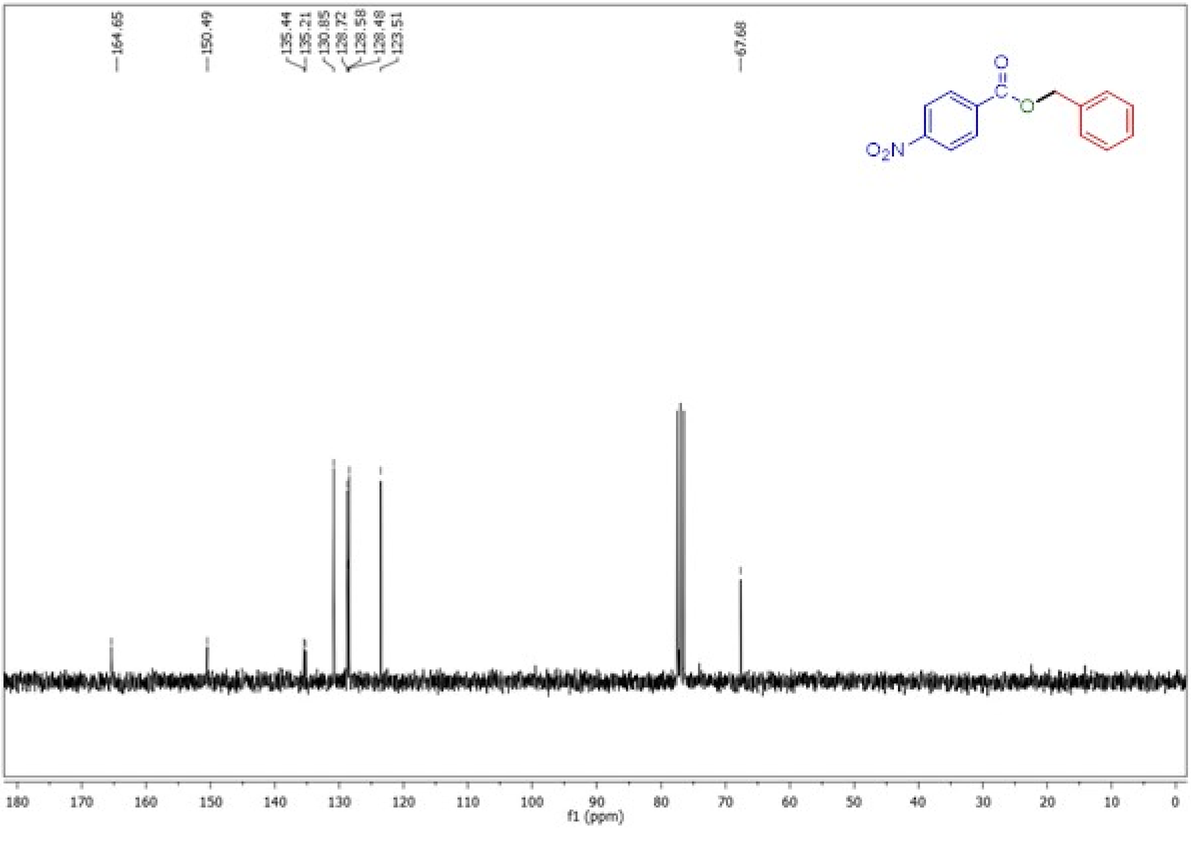

^{13}C-NMR of **3e**

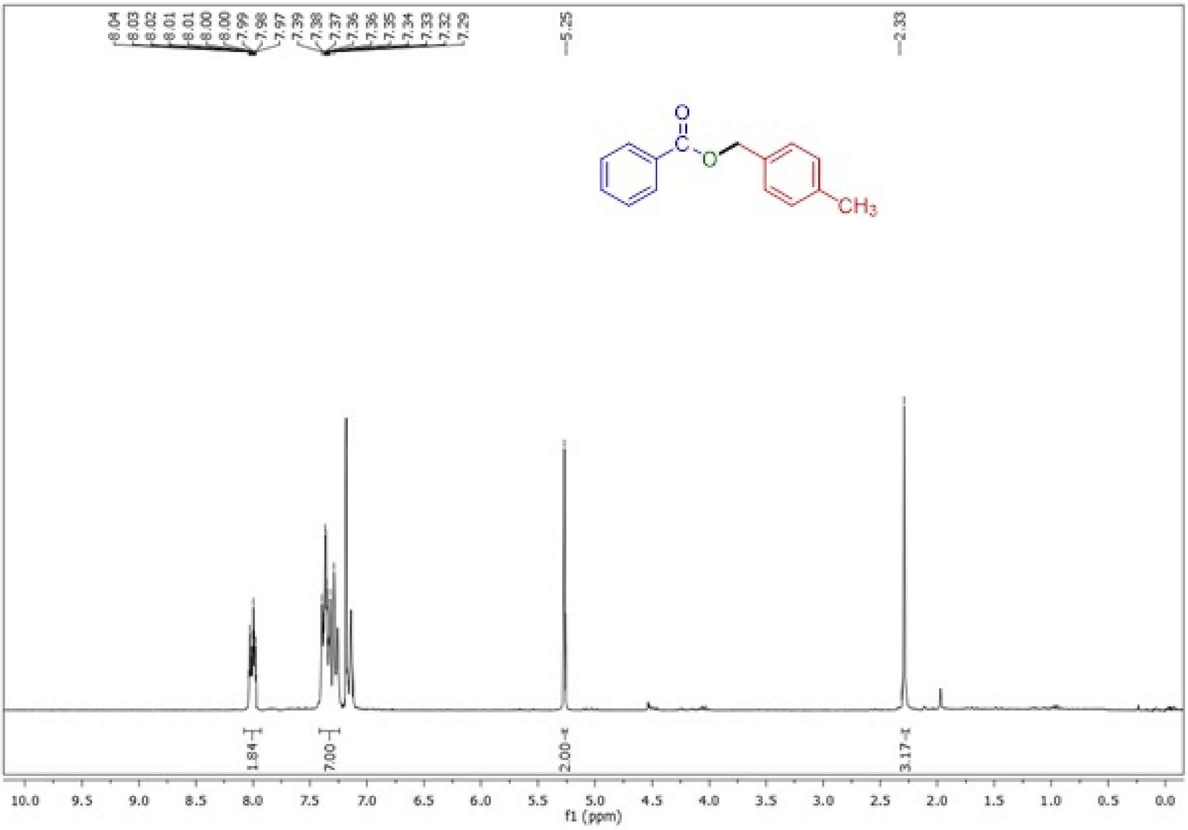

^{1}H-NMR of **3f**

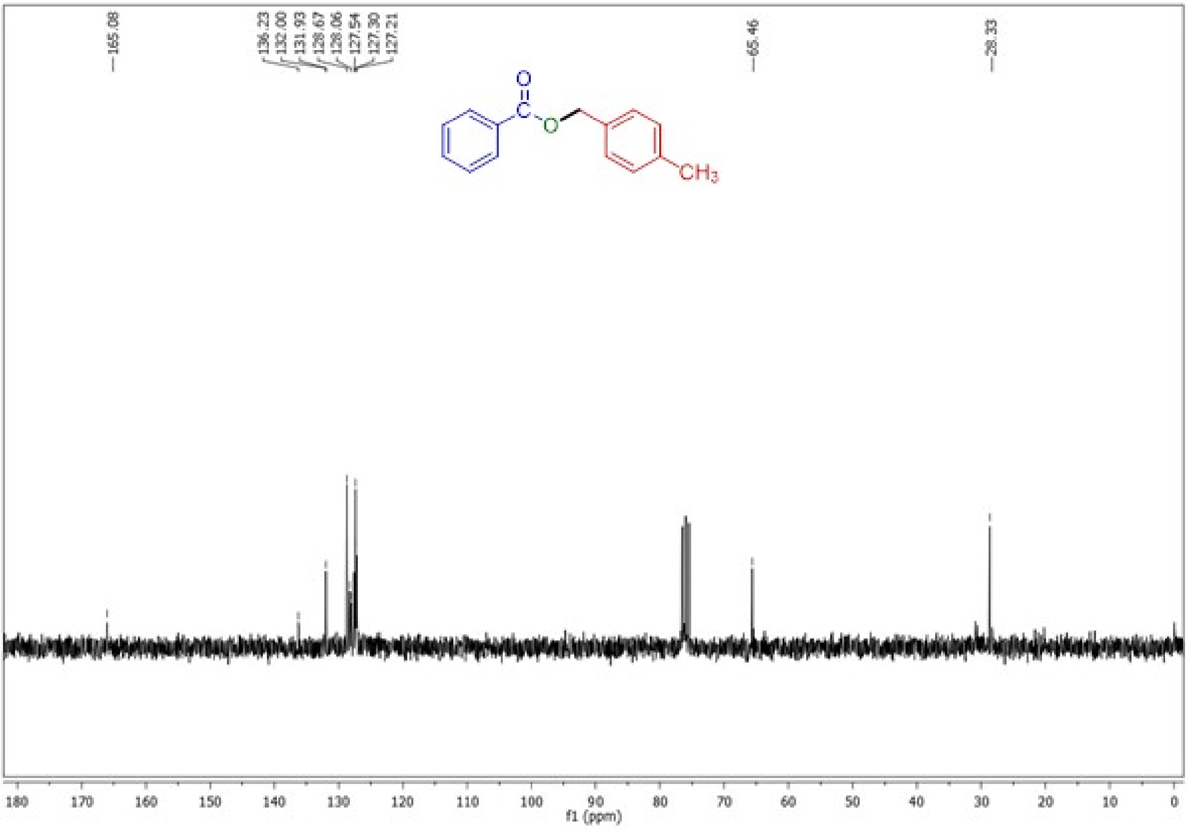

^{13}C-NMR of **3f**

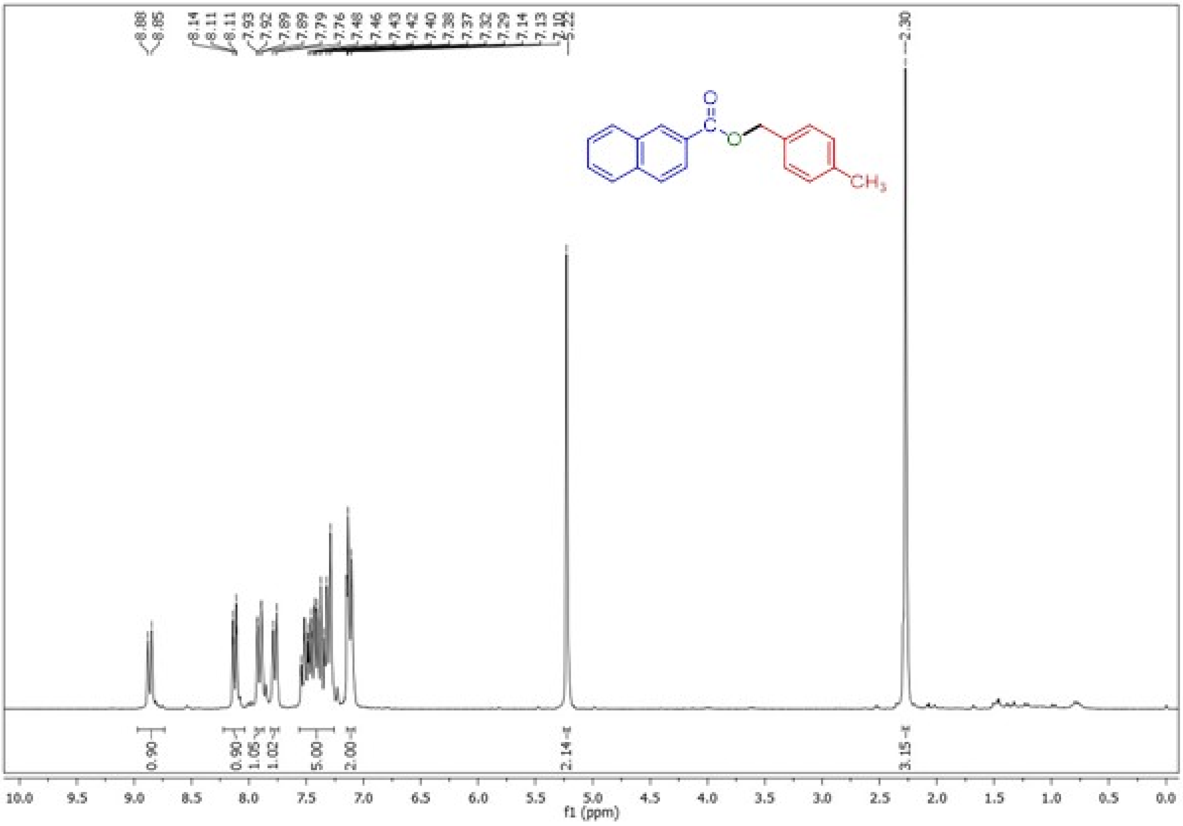

^{1}H-NMR of **3g**

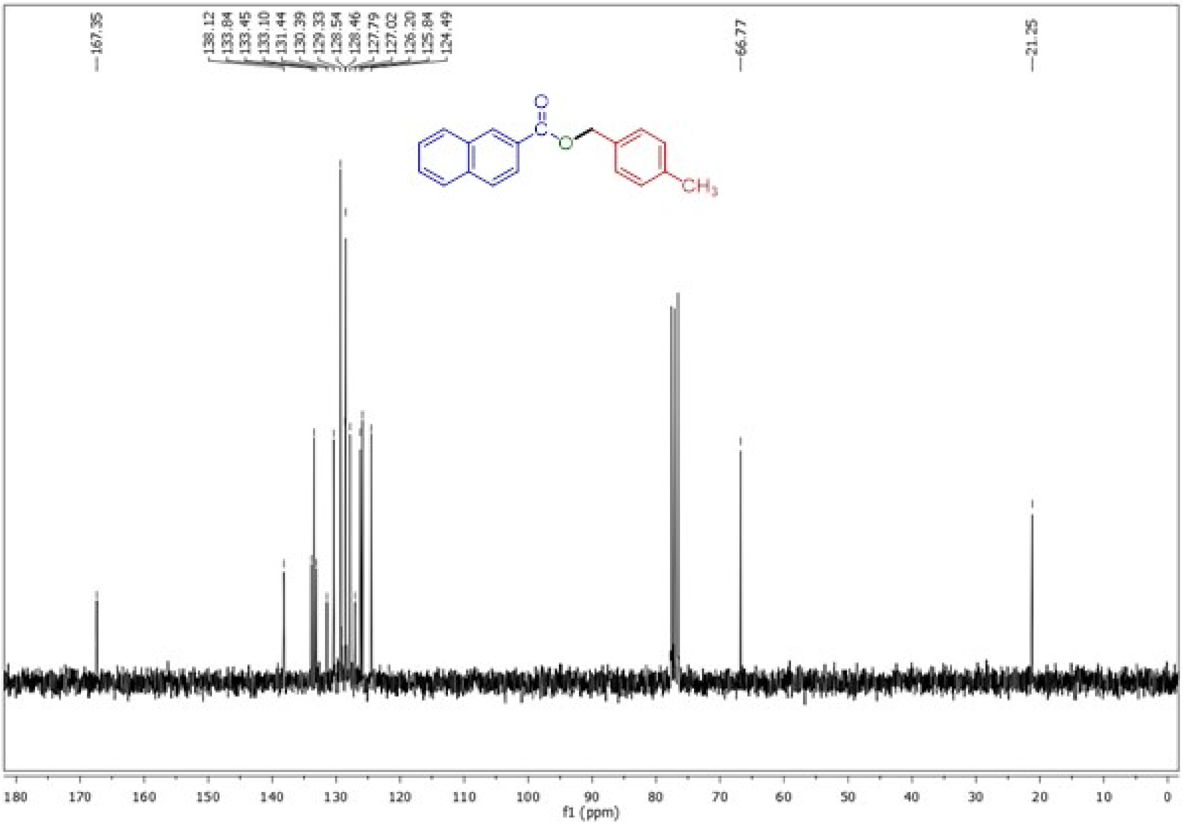

^{13}C-NMR of **3g**

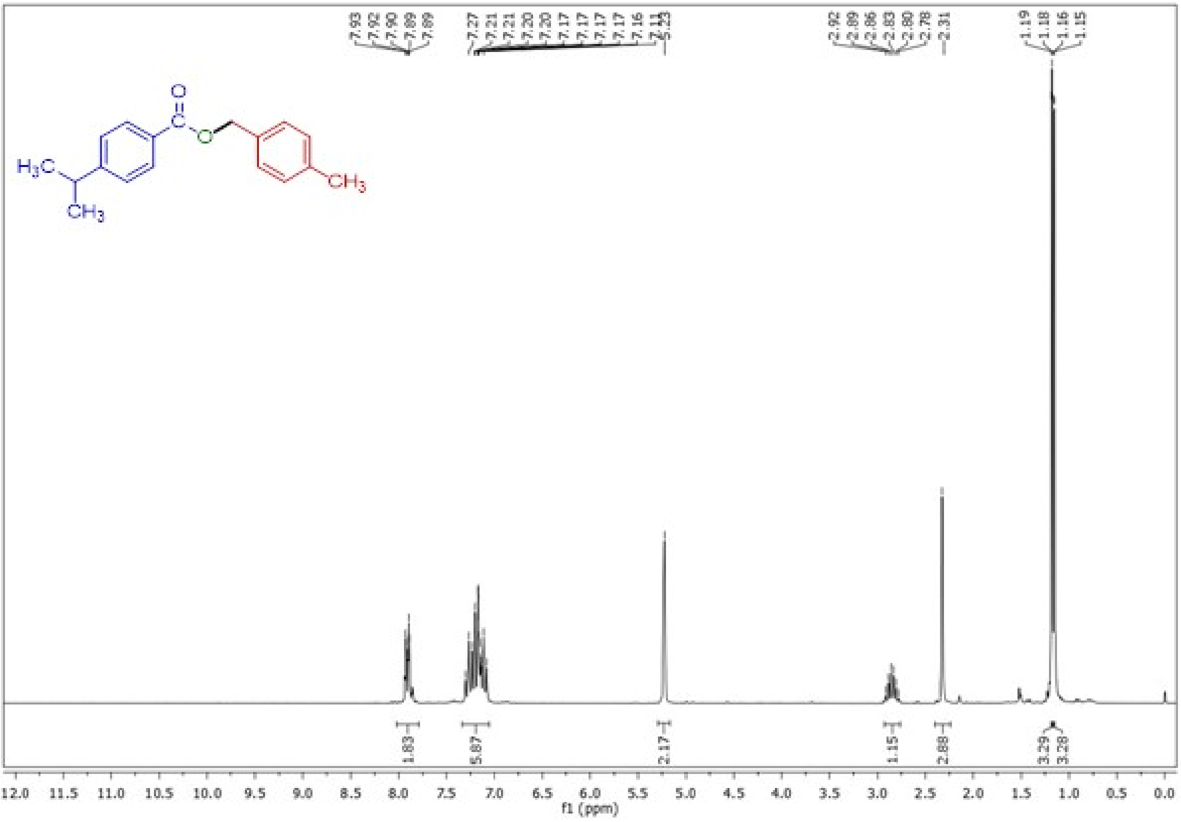

^{1}H-NMR of **3h**

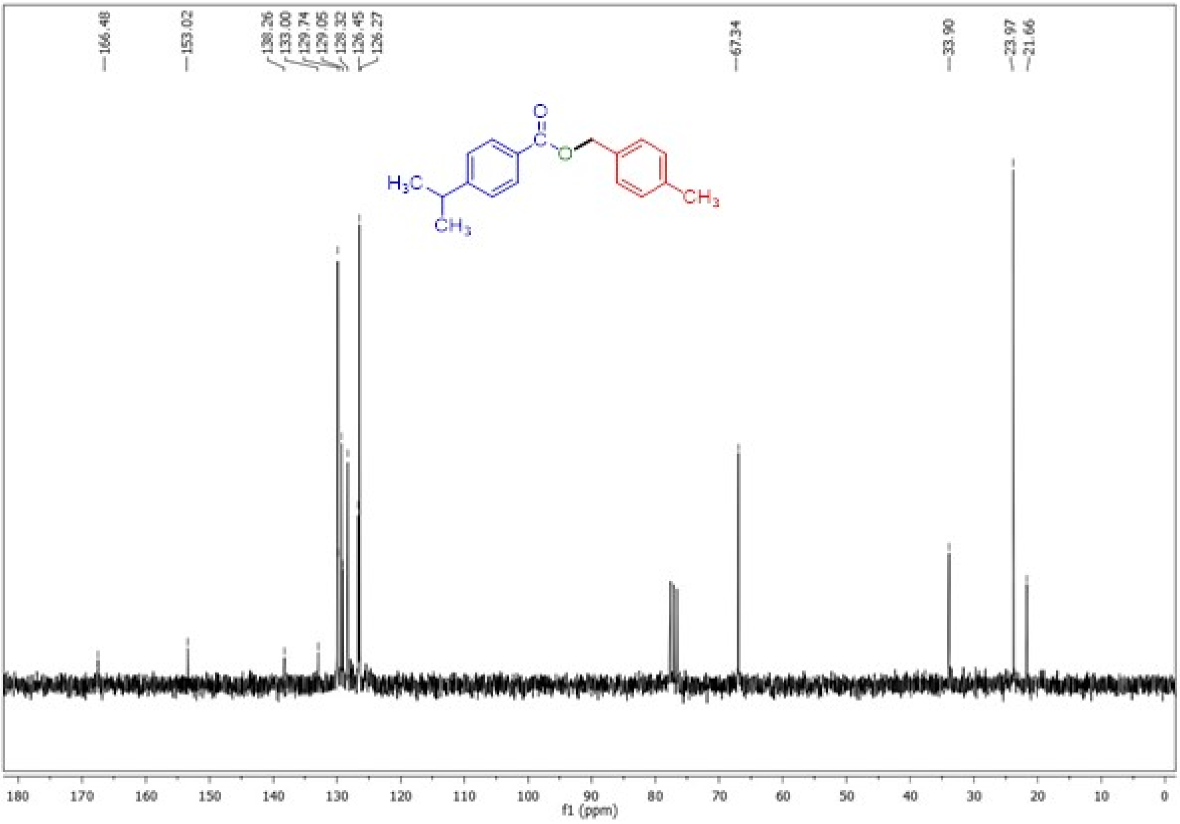

^{13}C-NMR of **3h**

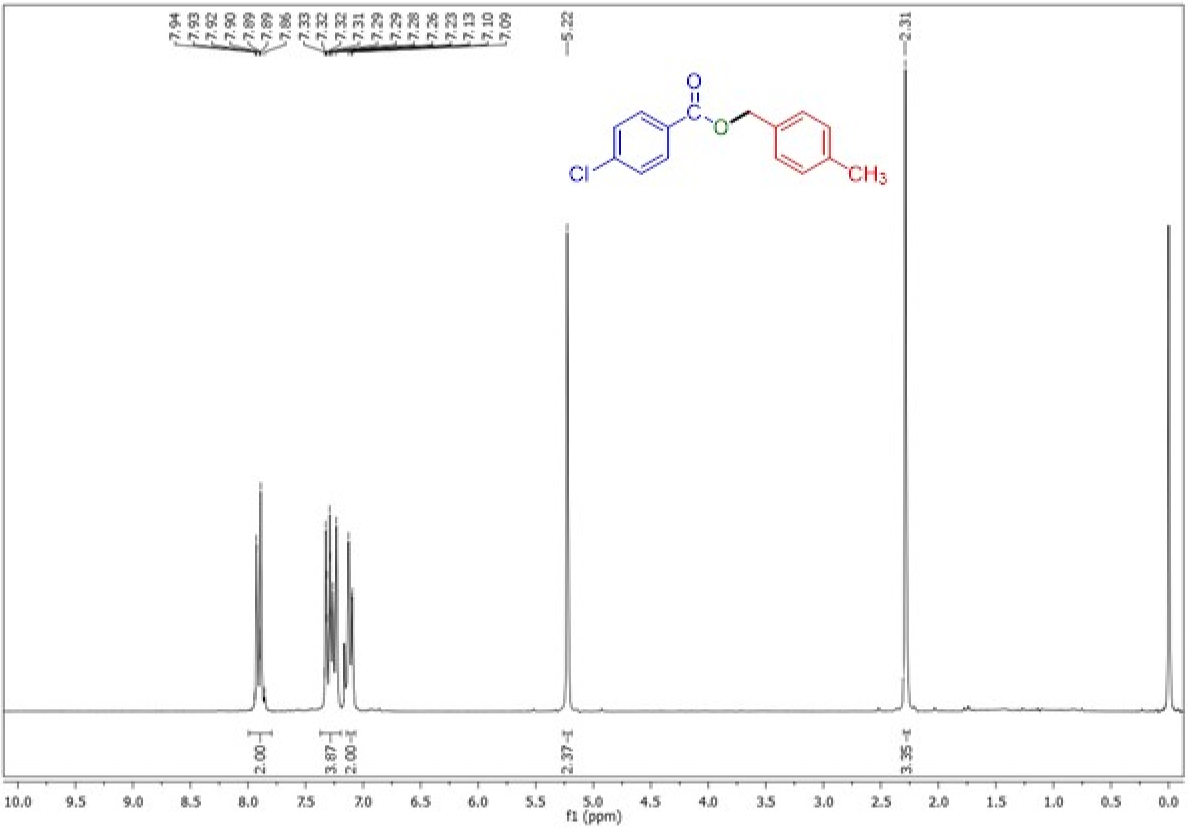

^{1}H-NMR of **3i**

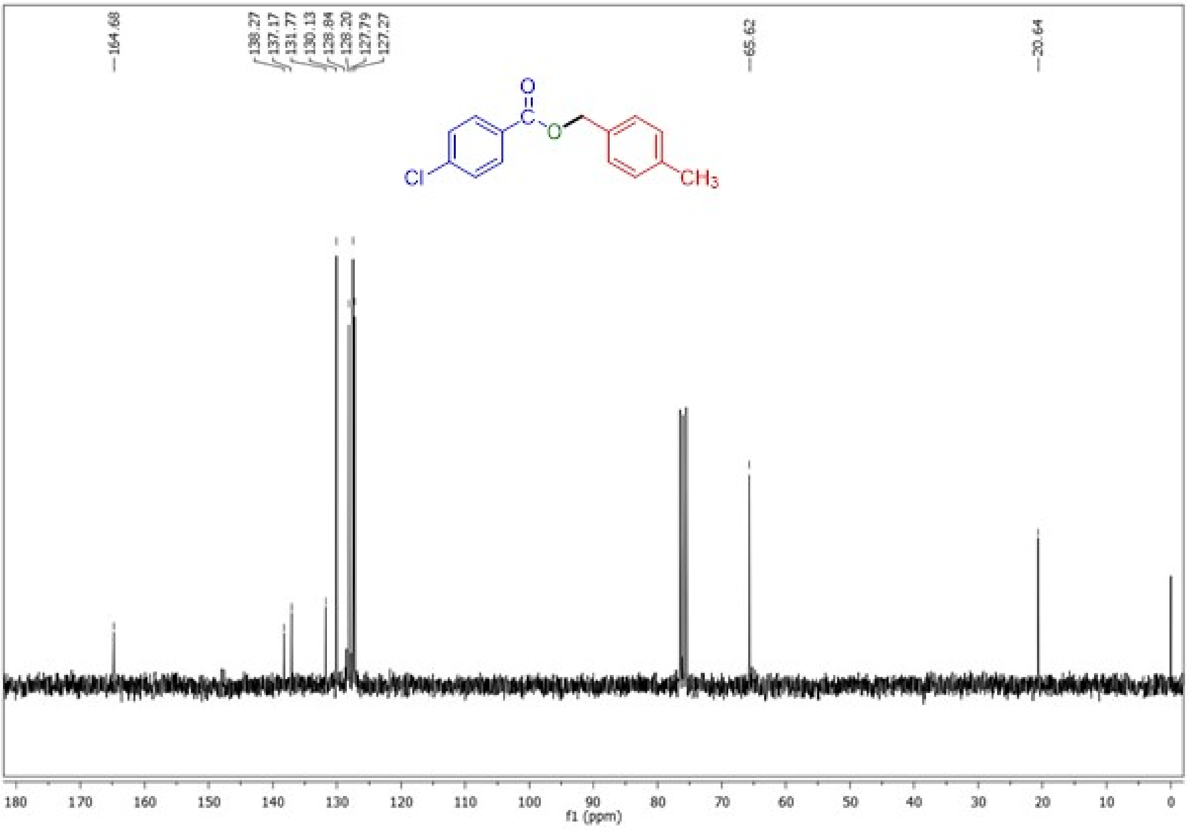

^{13}C-NMR of **3i**

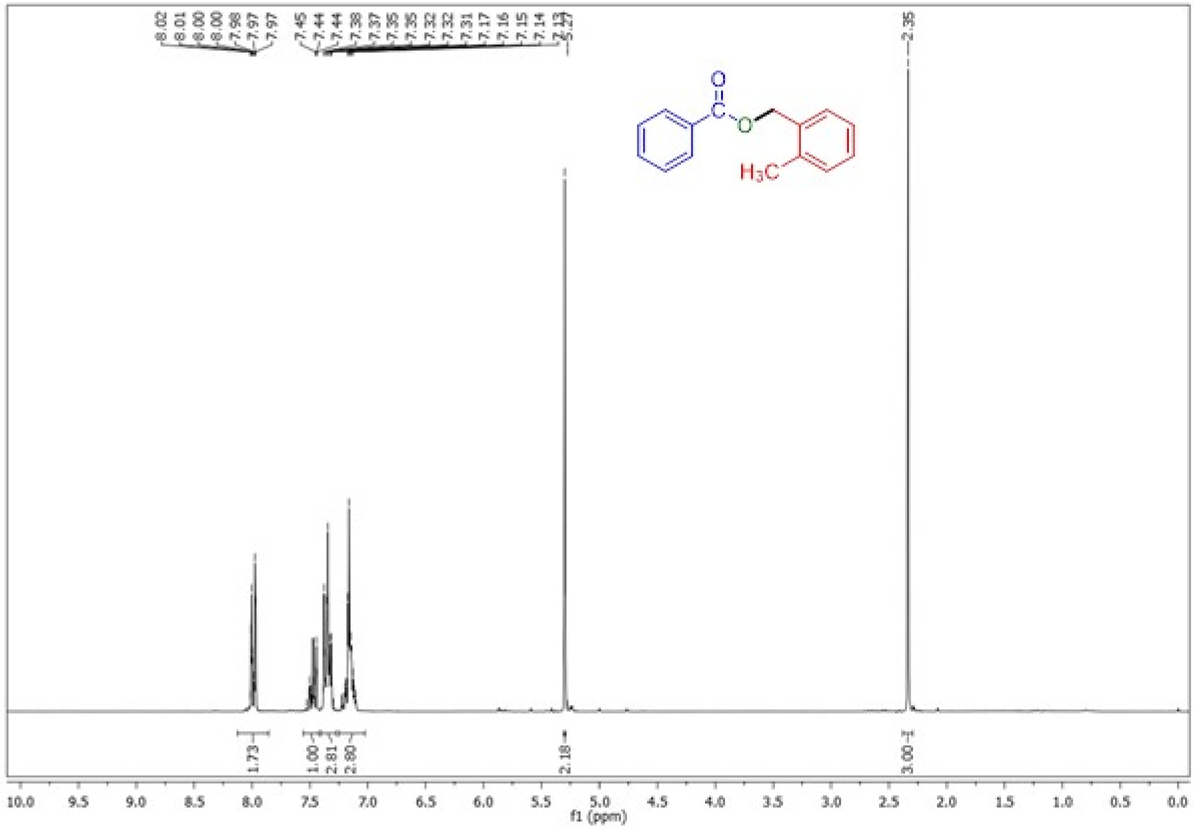

^{1}H-NMR of **3j**

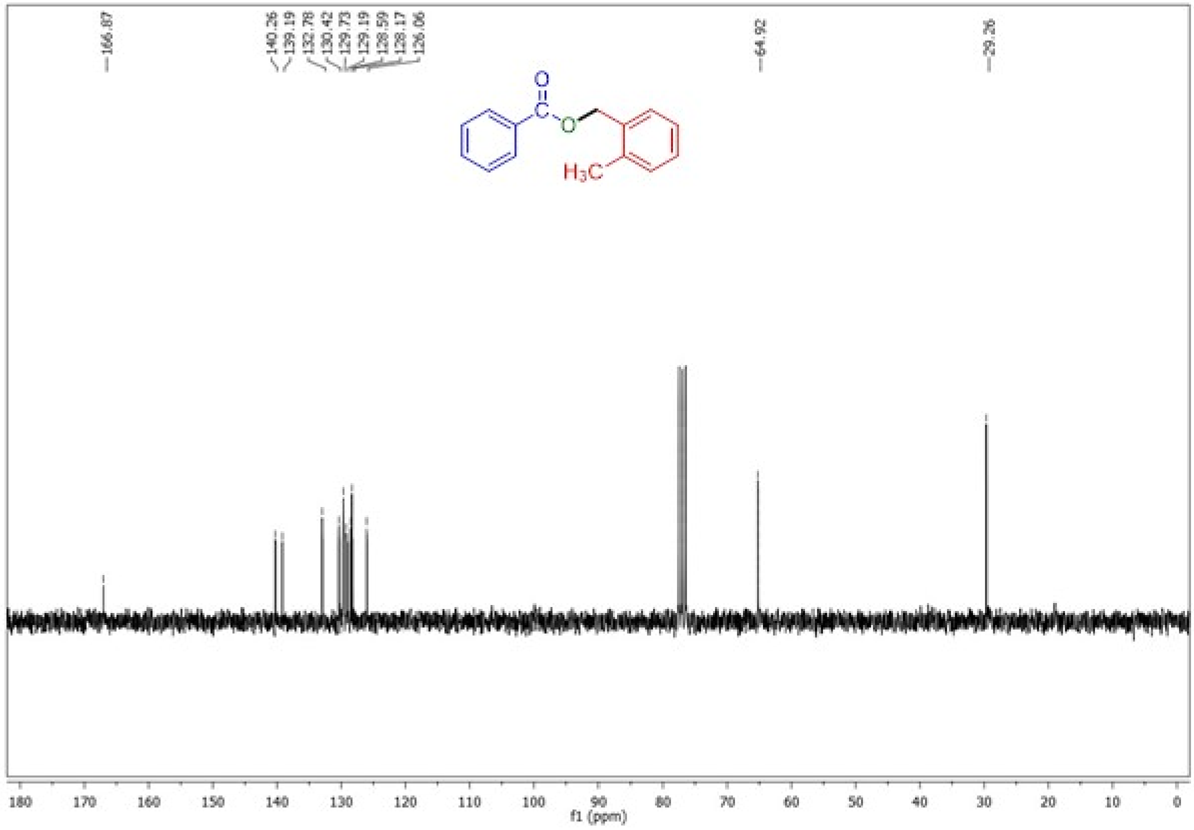

^{13}C-NMR of **3j**

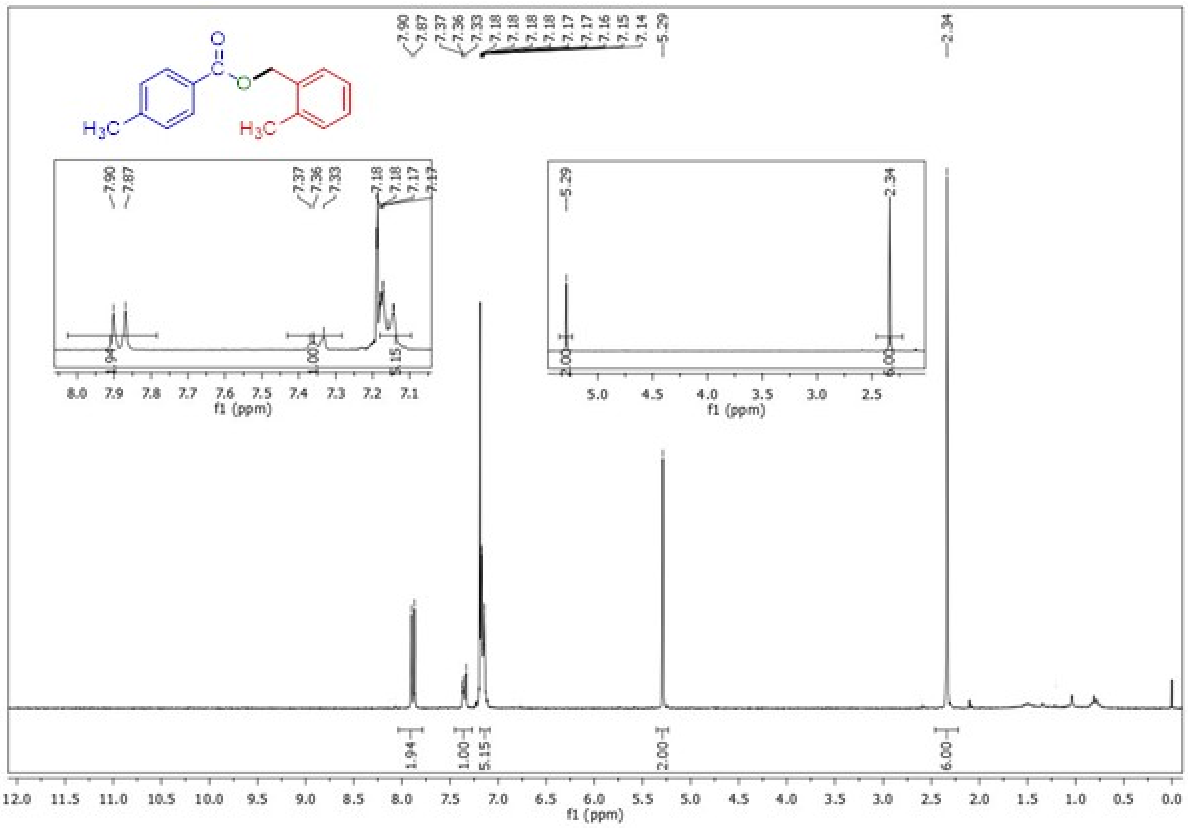

^{1}H-NMR of **3k**

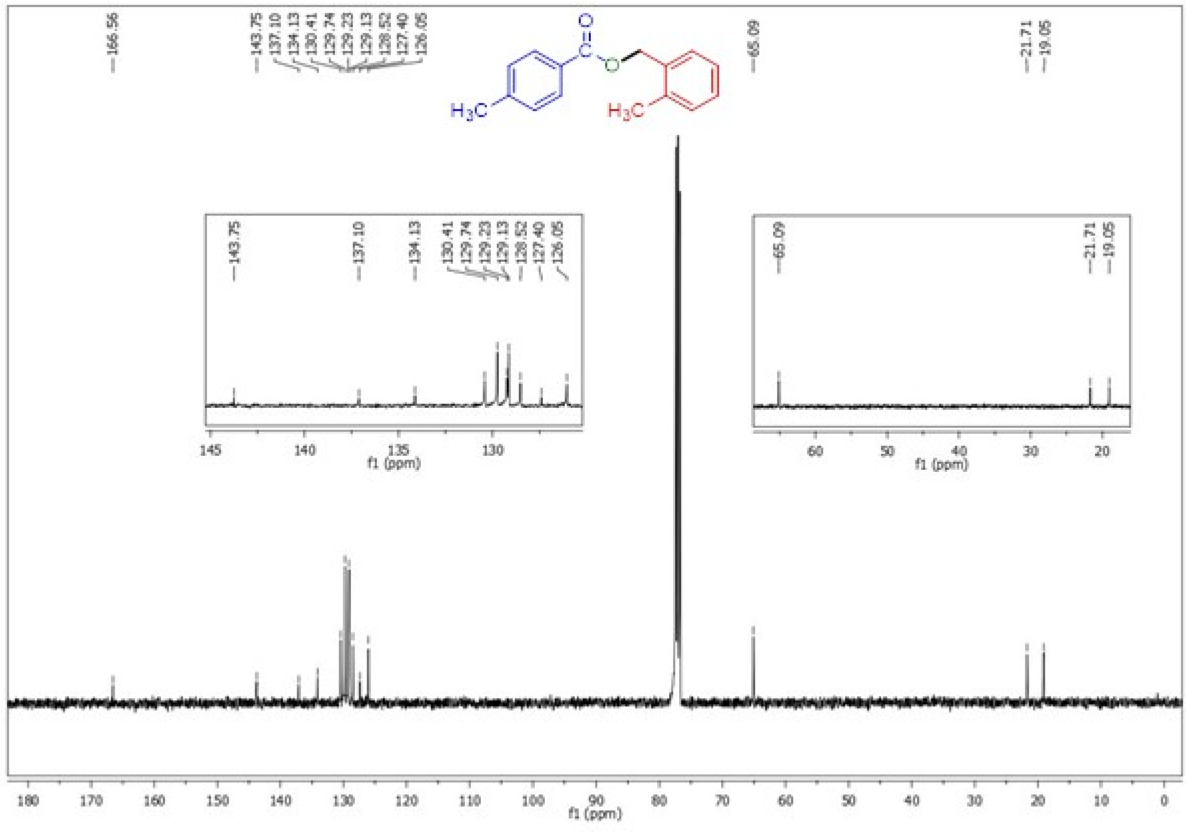

^{13}C-NMR of **3k**

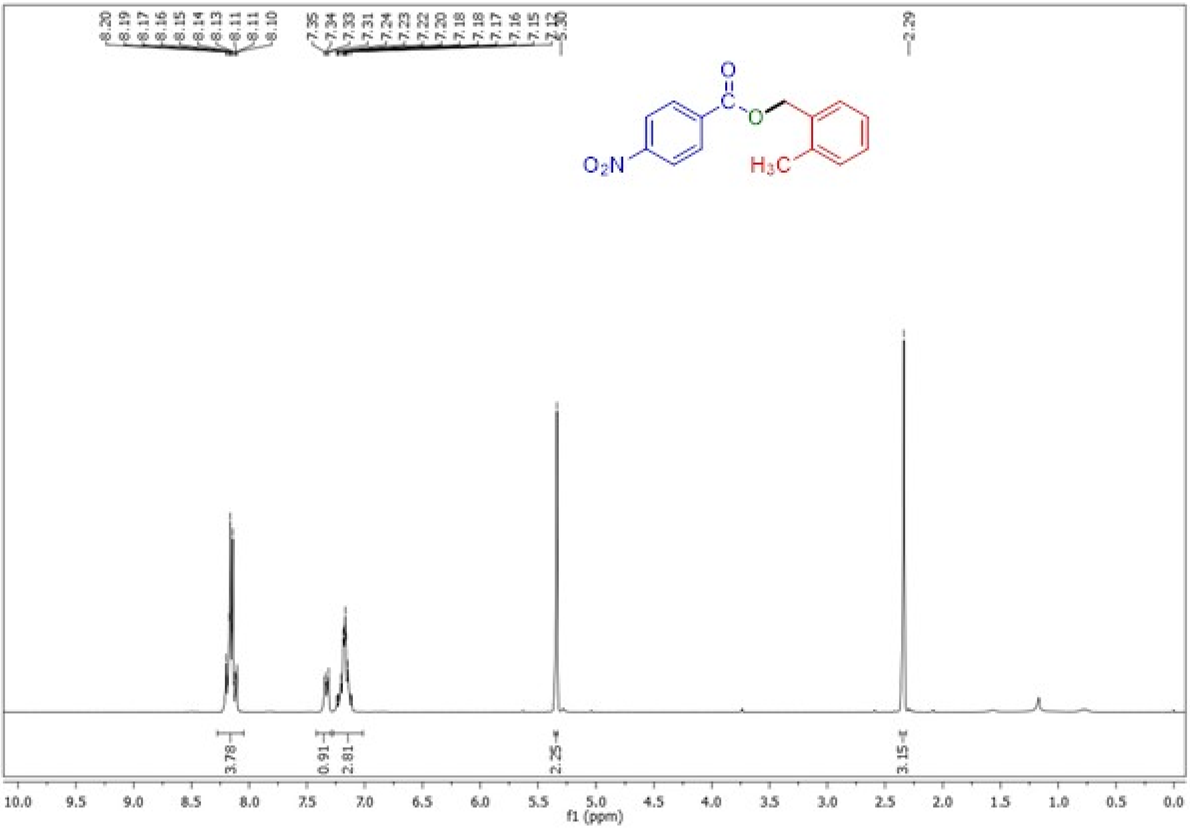

^{1}H-NMR of **3l**

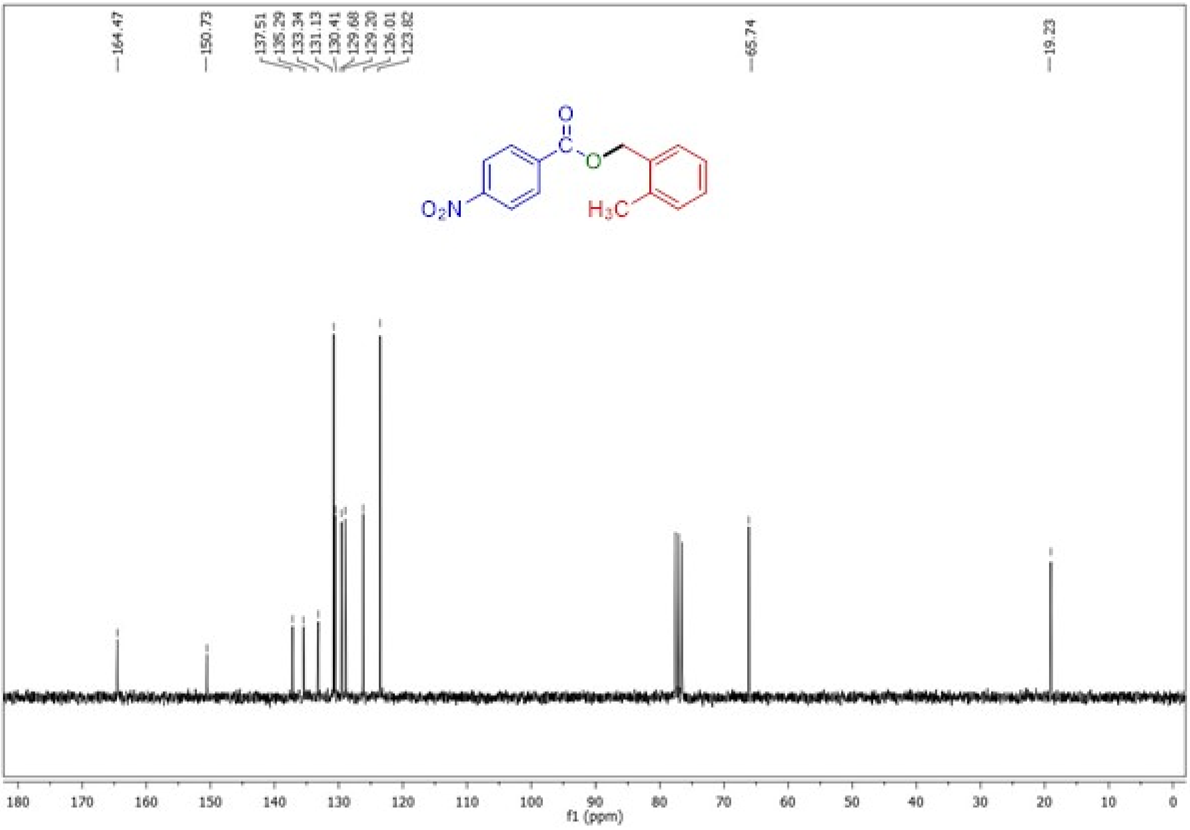

^{13}C-NMR of **3l**

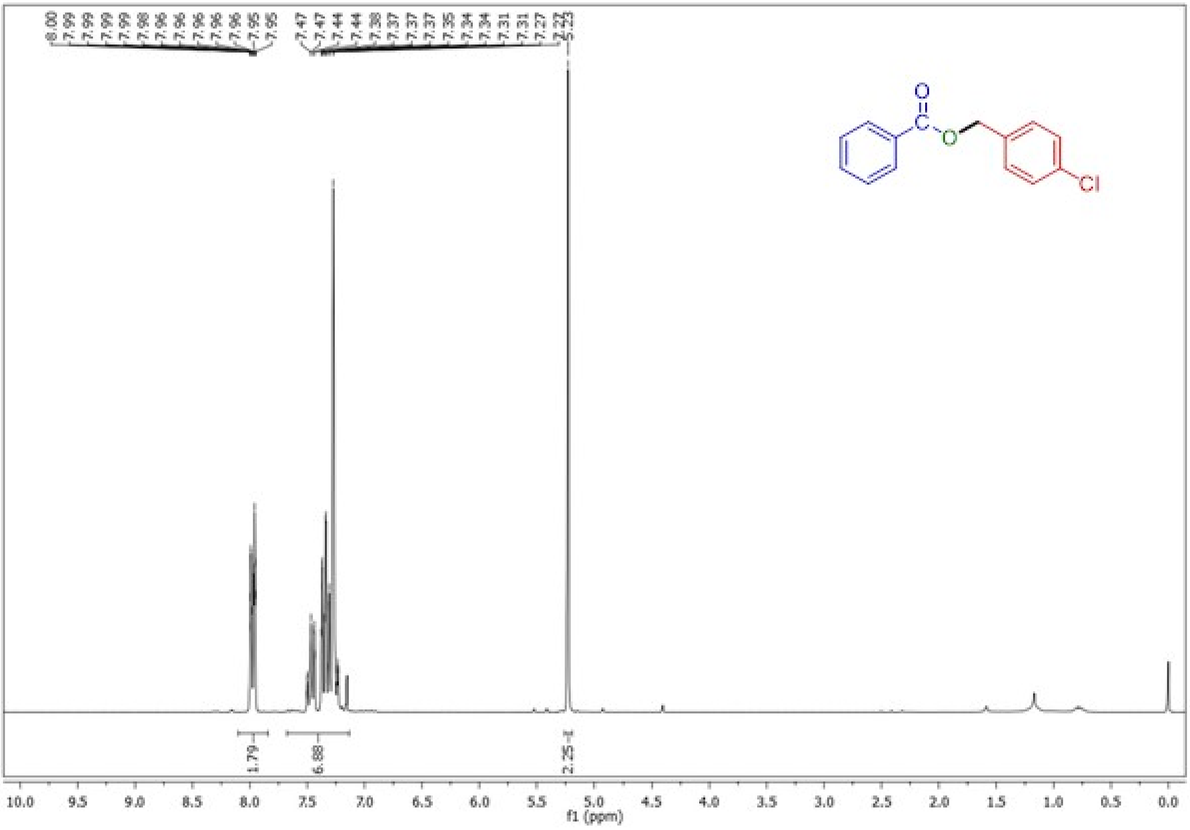

^{1}H-NMR of **3m**

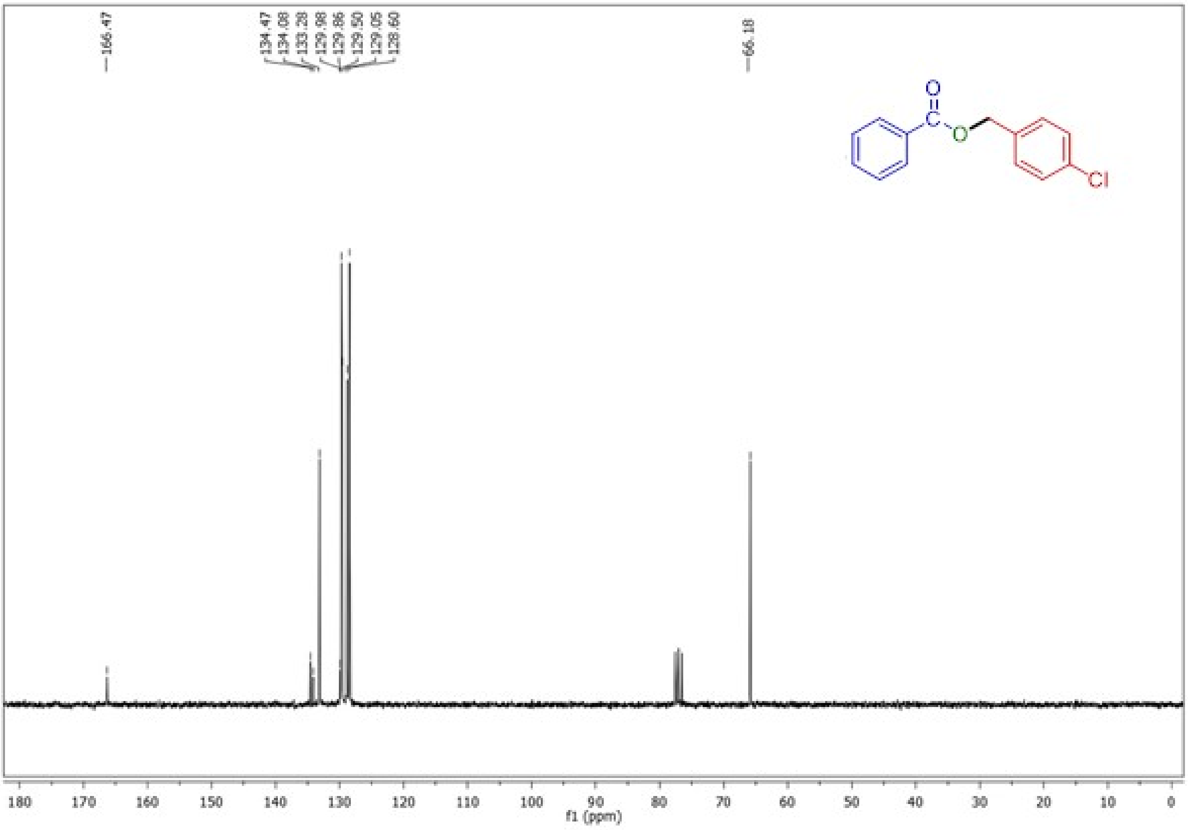

^{13}C-NMR of **3m**

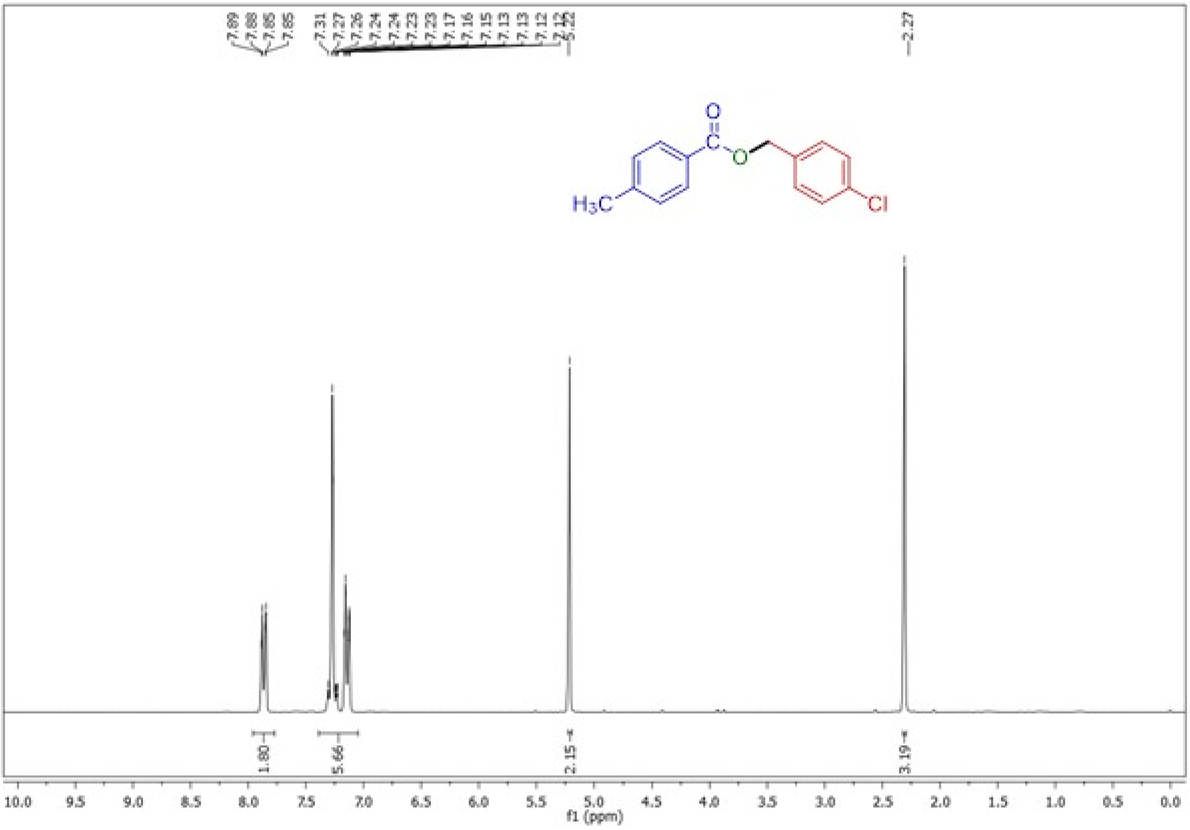

^{1}H-NMR of **3n**

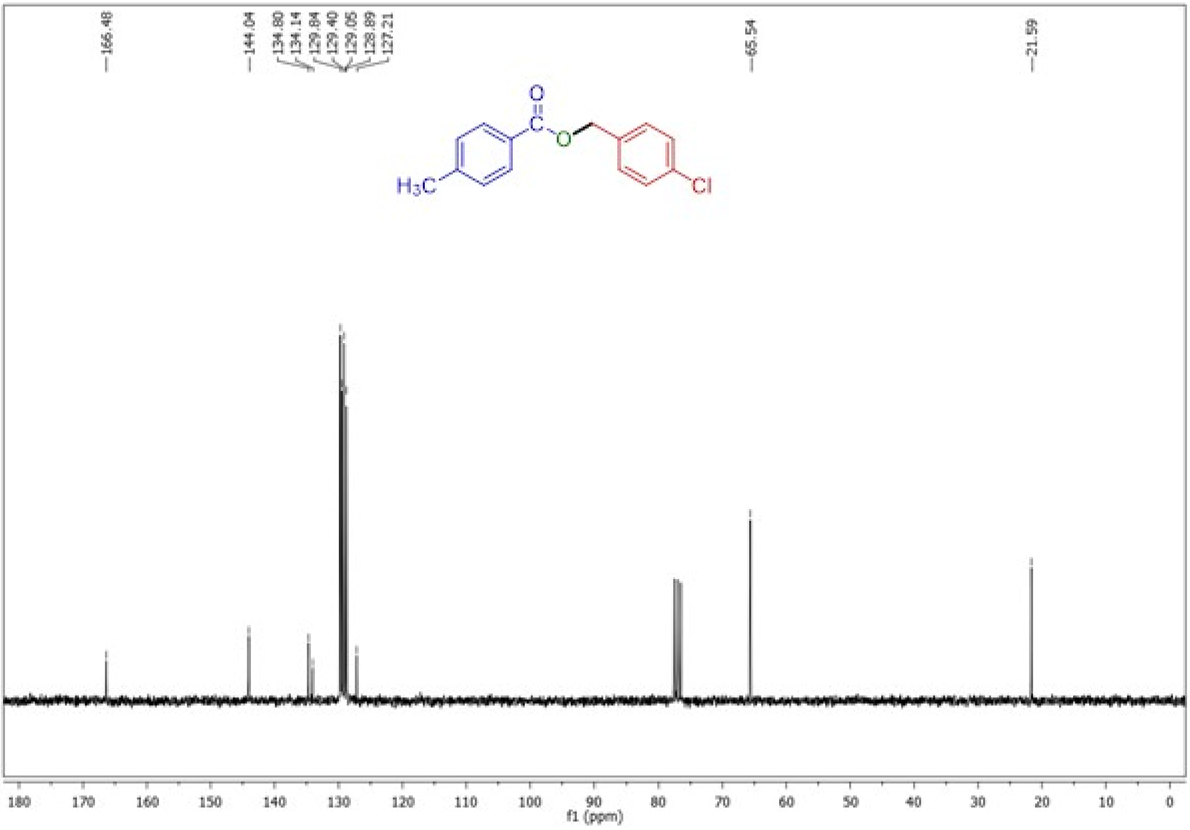

^{13}C-NMR of **3n**

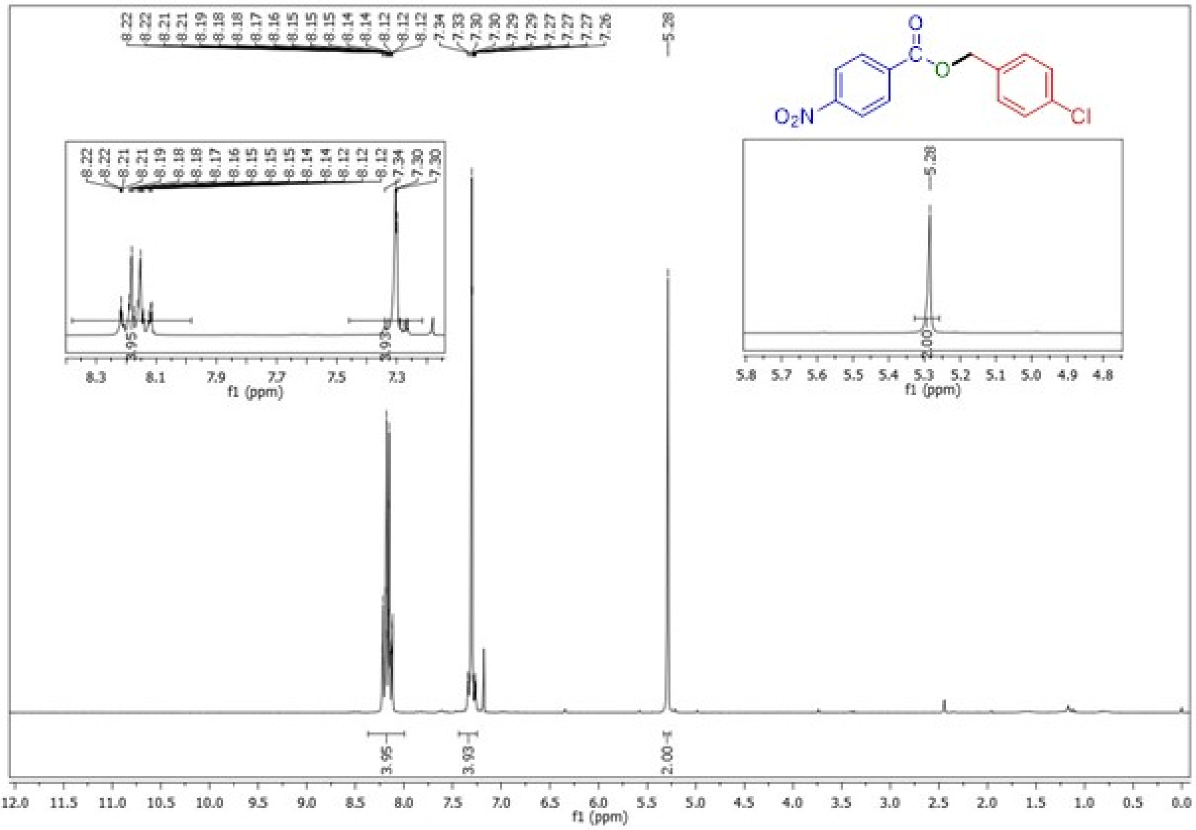

^{1}H-NMR of **3o**

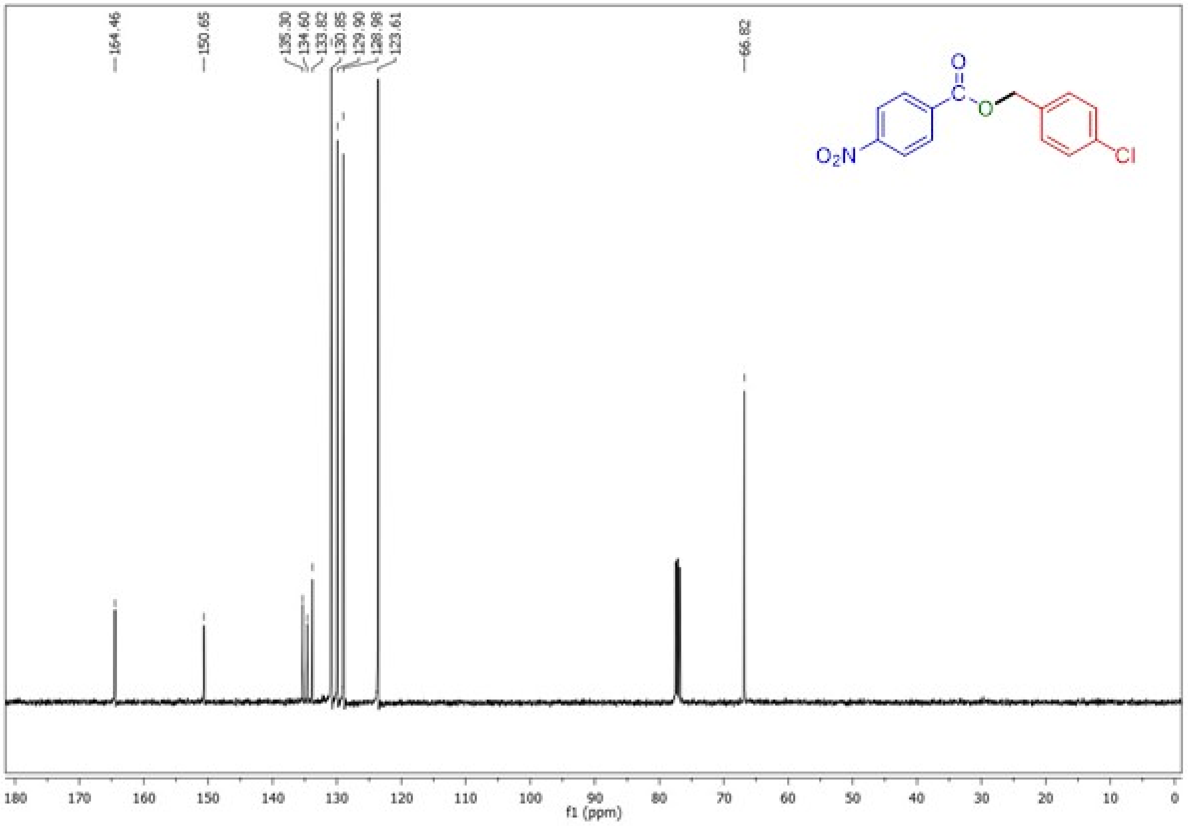

^{13}C-NMR of **3o**

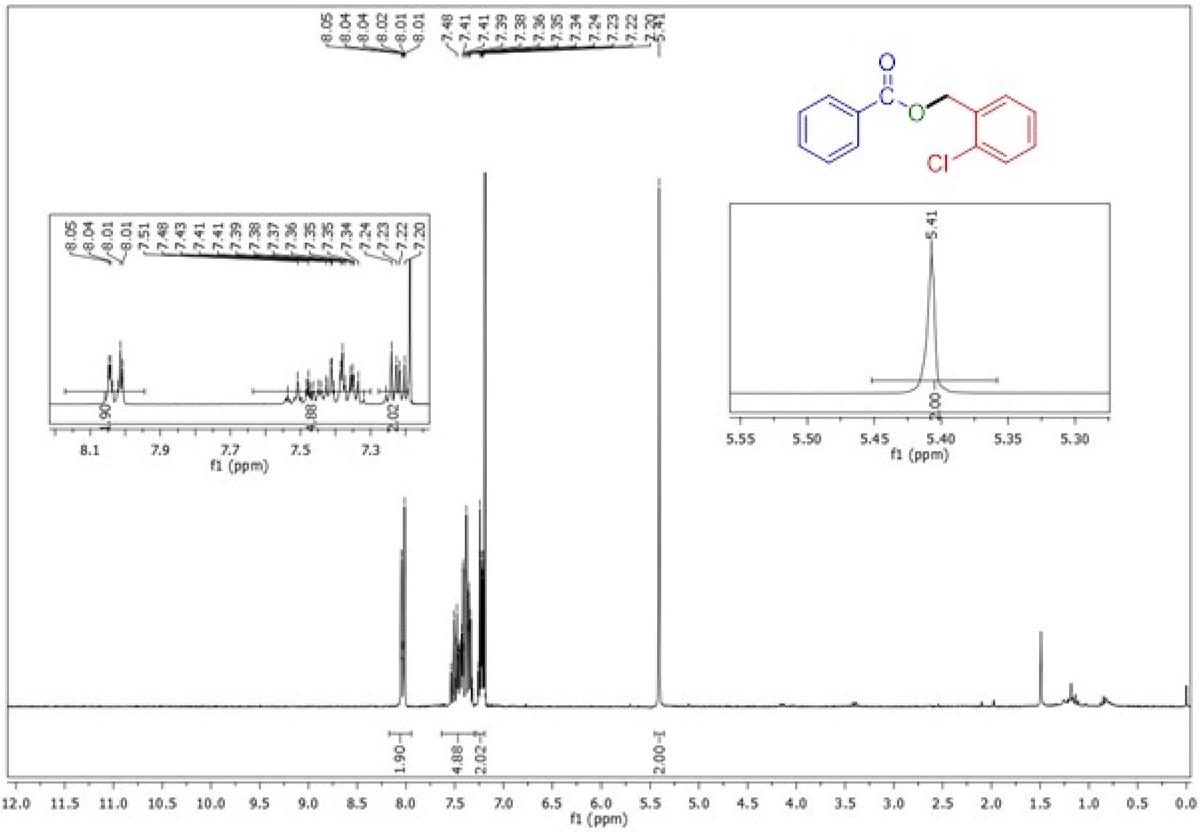

¹H-NMR of **3p**

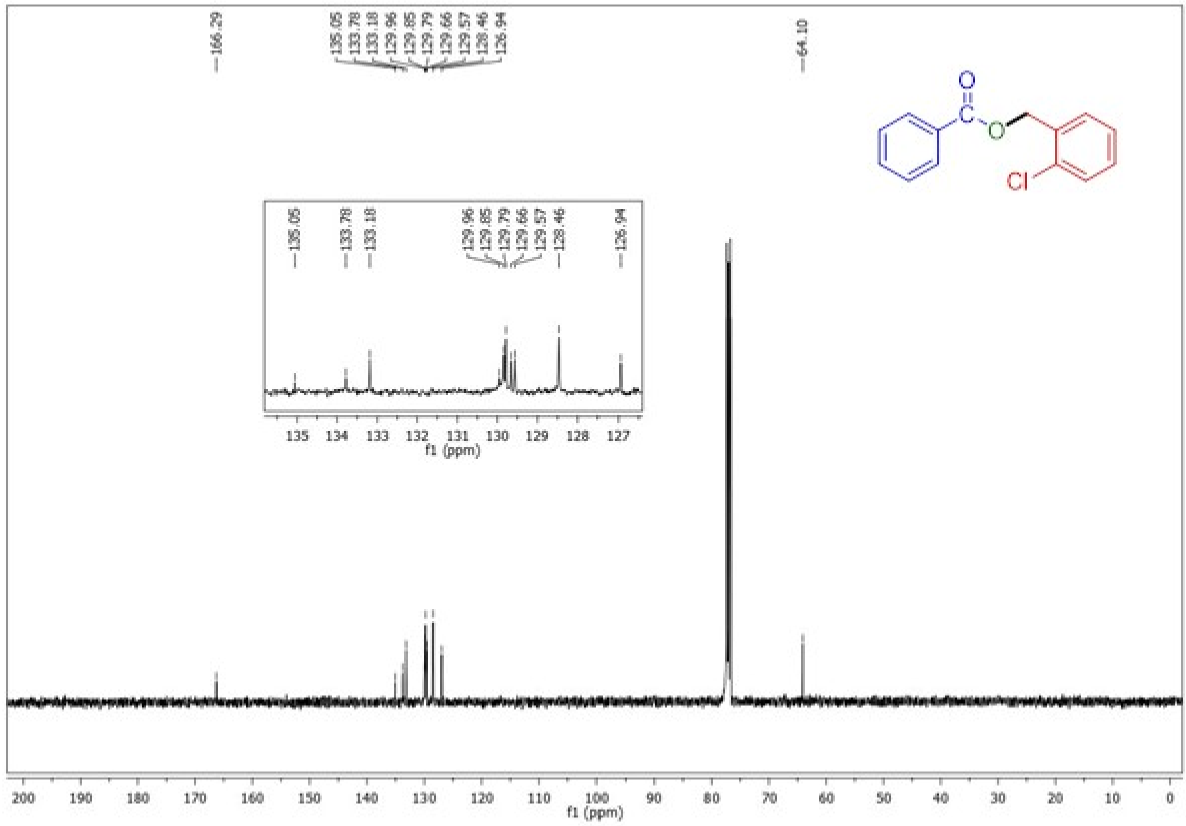

¹³C-NMR of **3p**

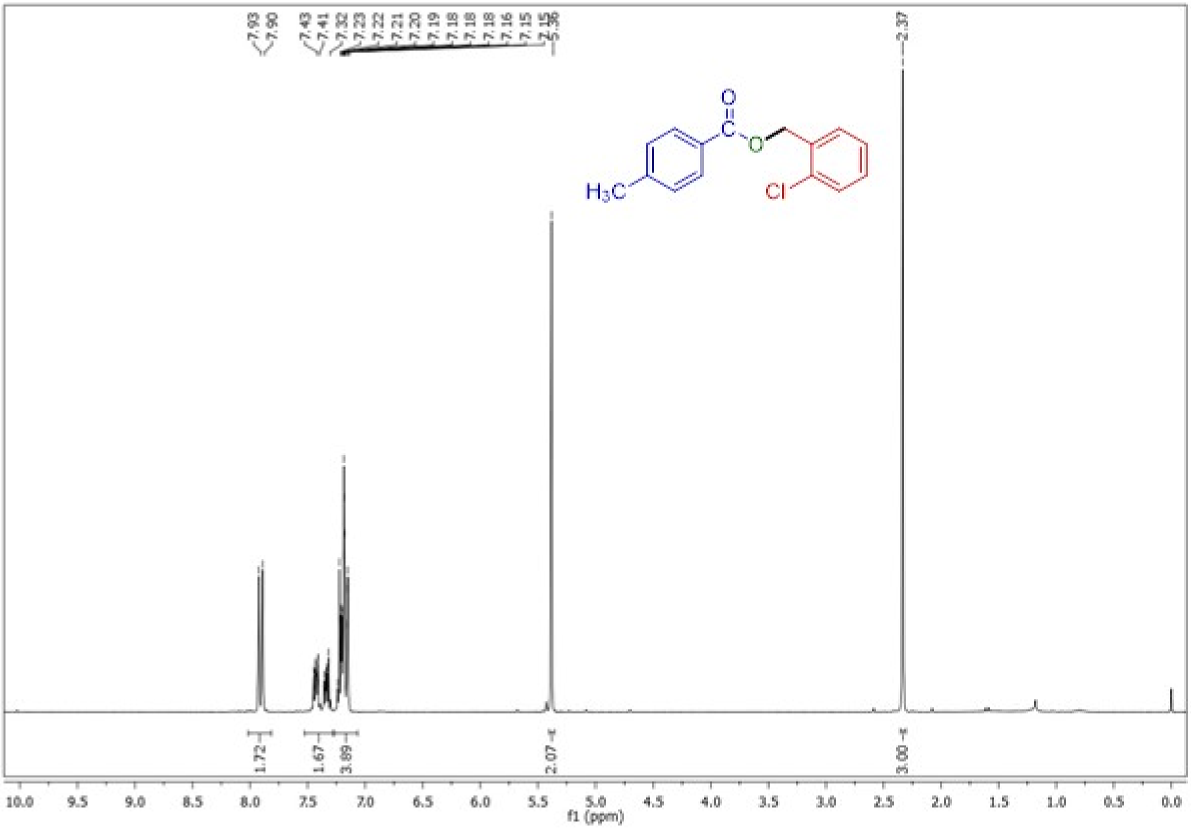

^{1}H-NMR of **3q**

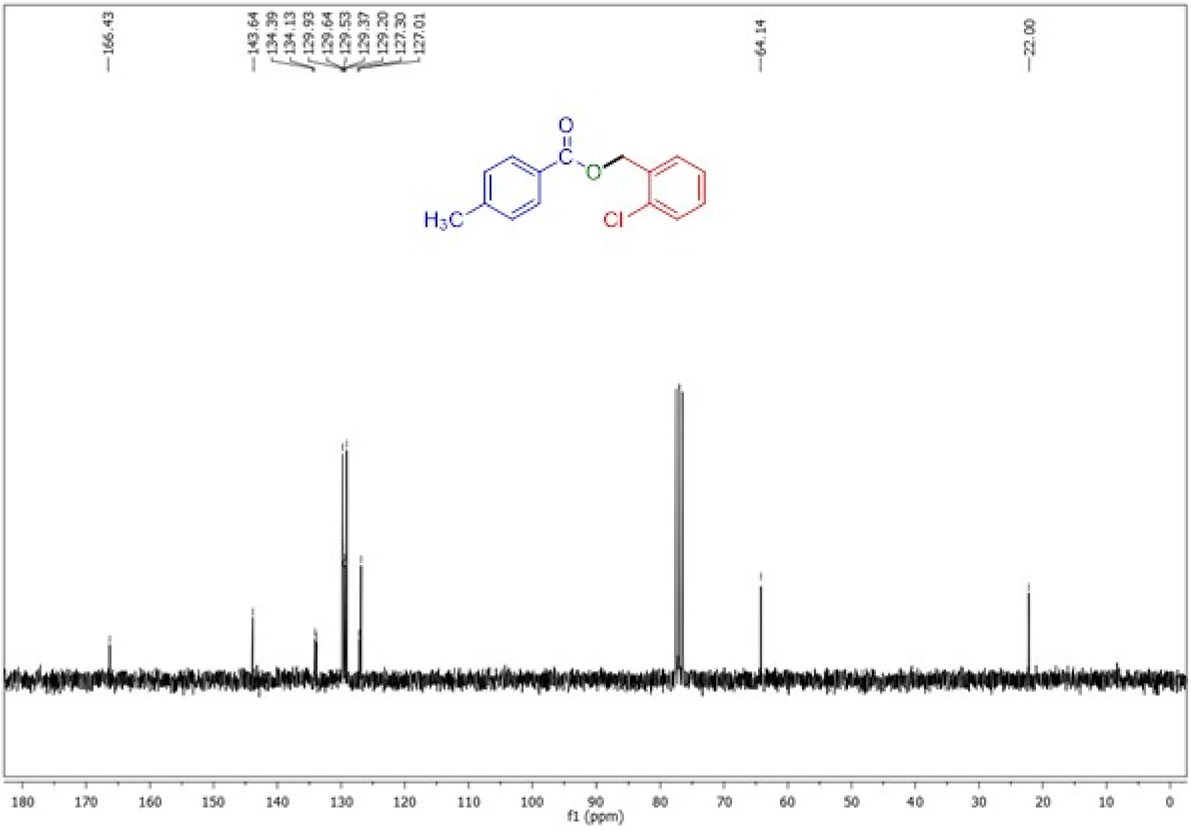

^{13}C-NMR of **3q**

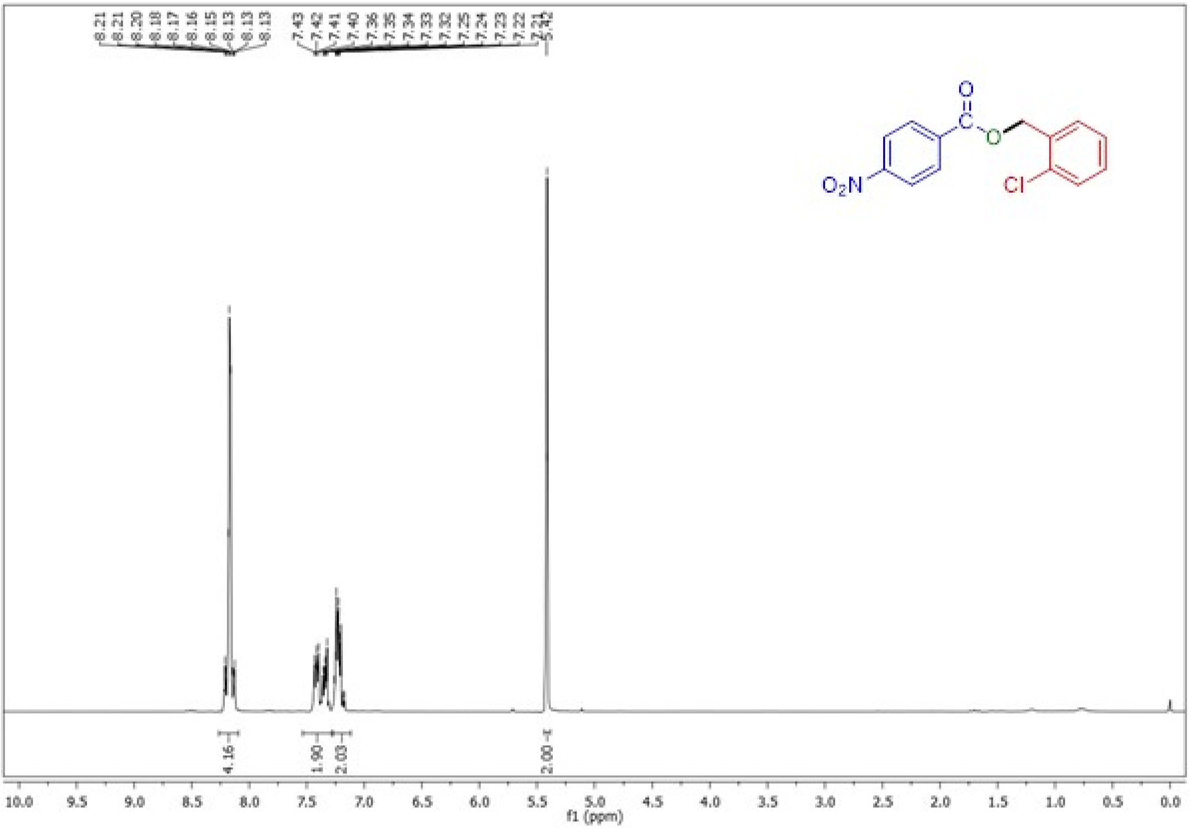

^{1}H-NMR of **3r**

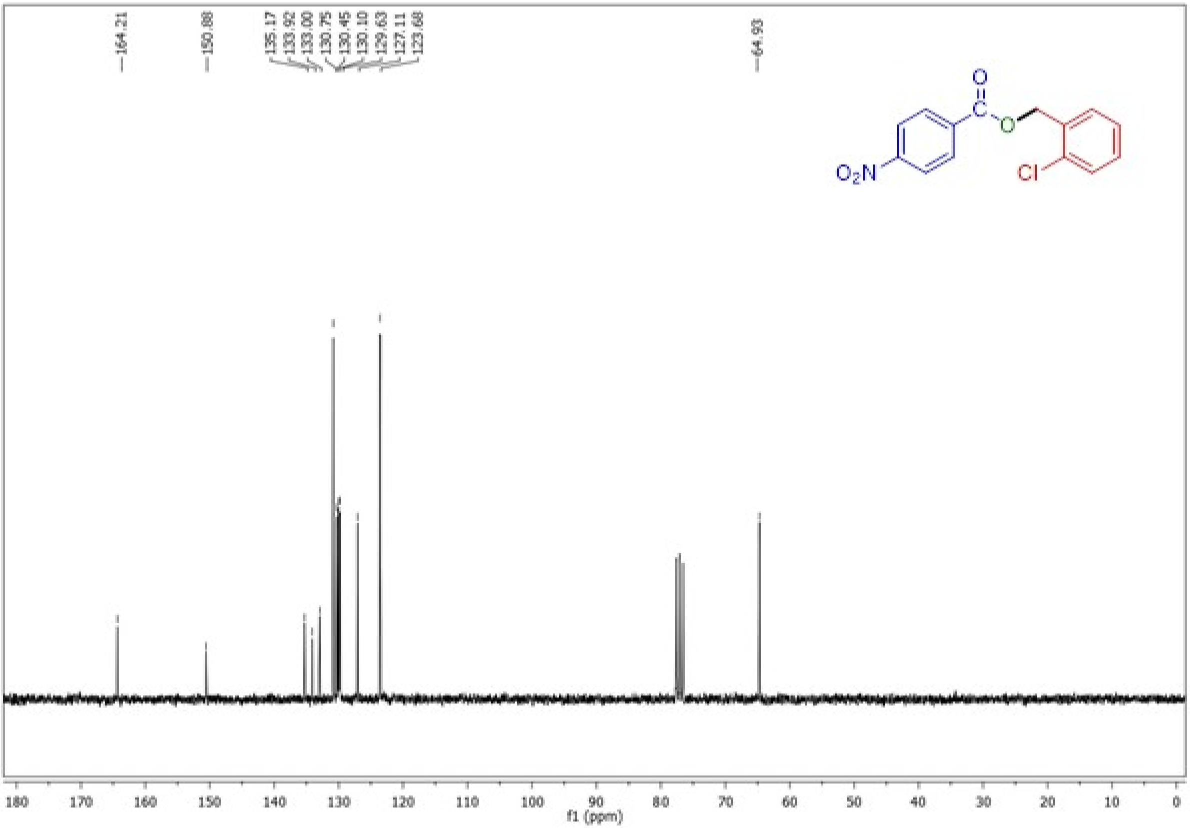

^{13}C-NMR of **3r**

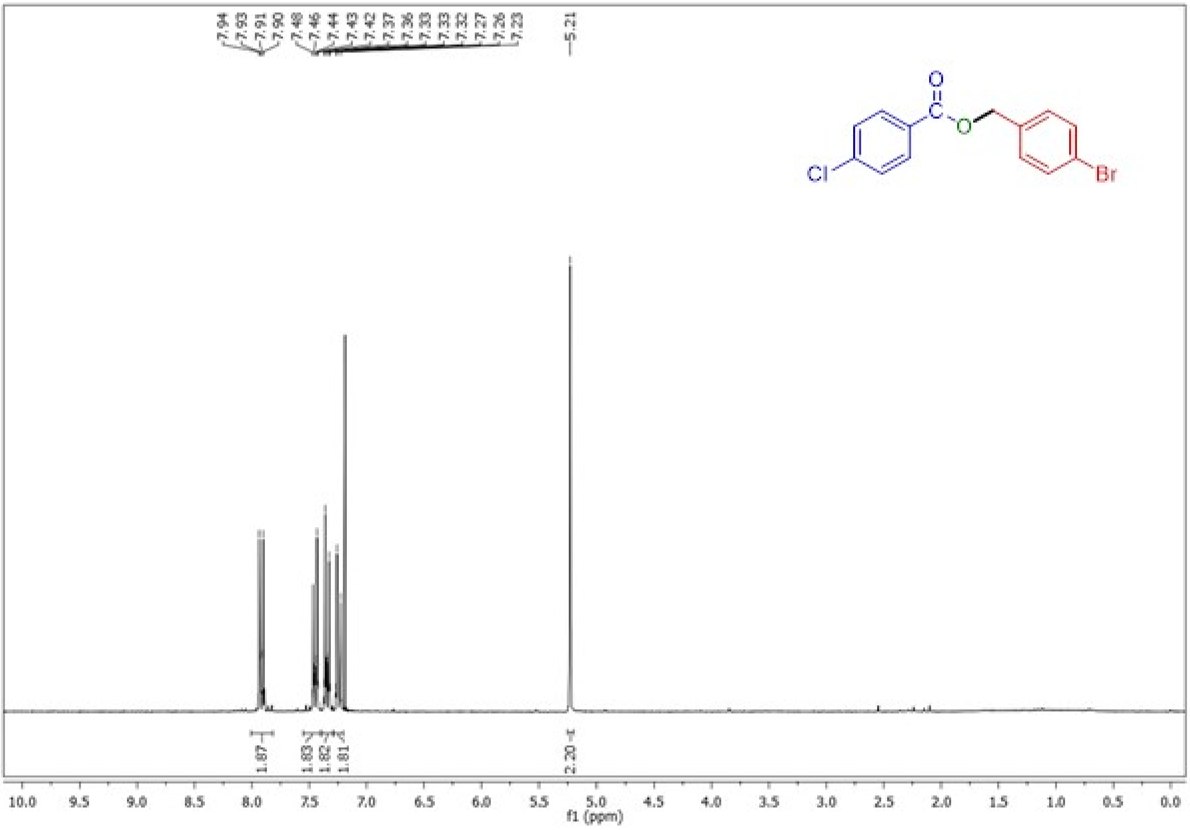

^{1}H-NMR of **3s**

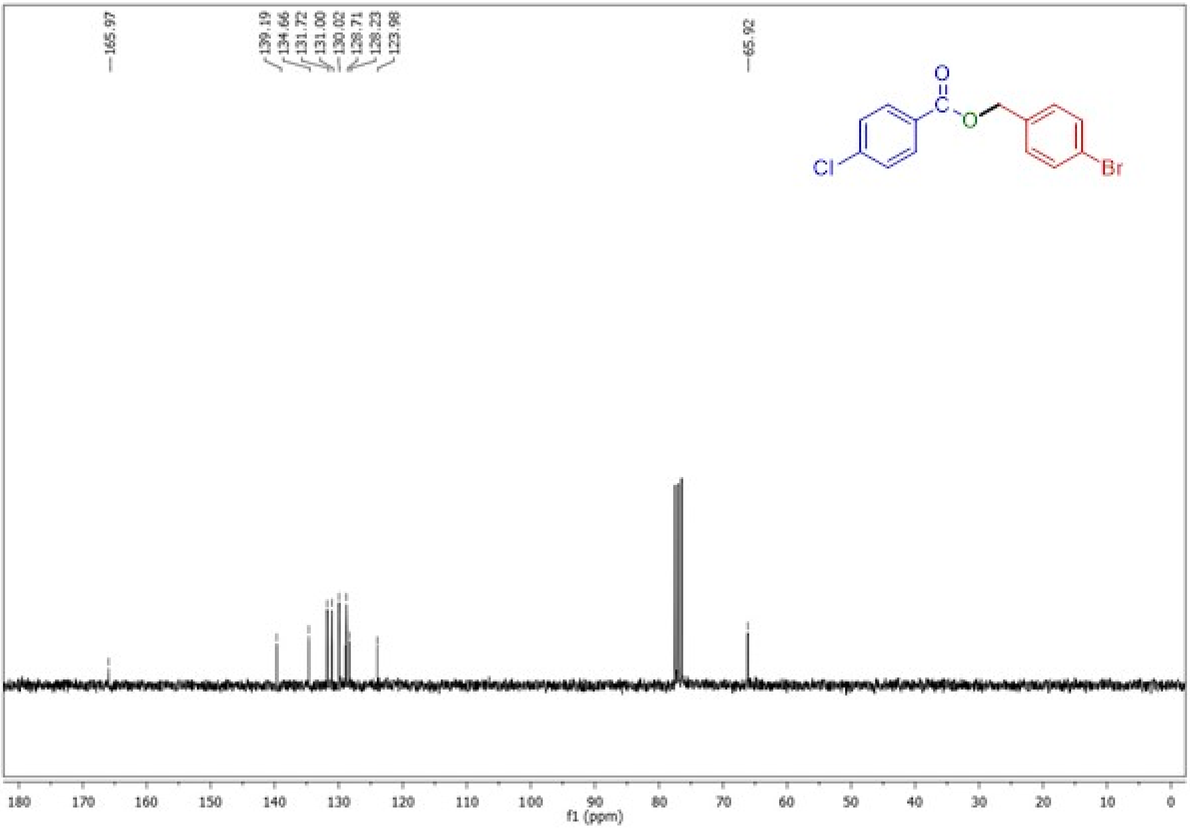

^{13}C-NMR of **3s**

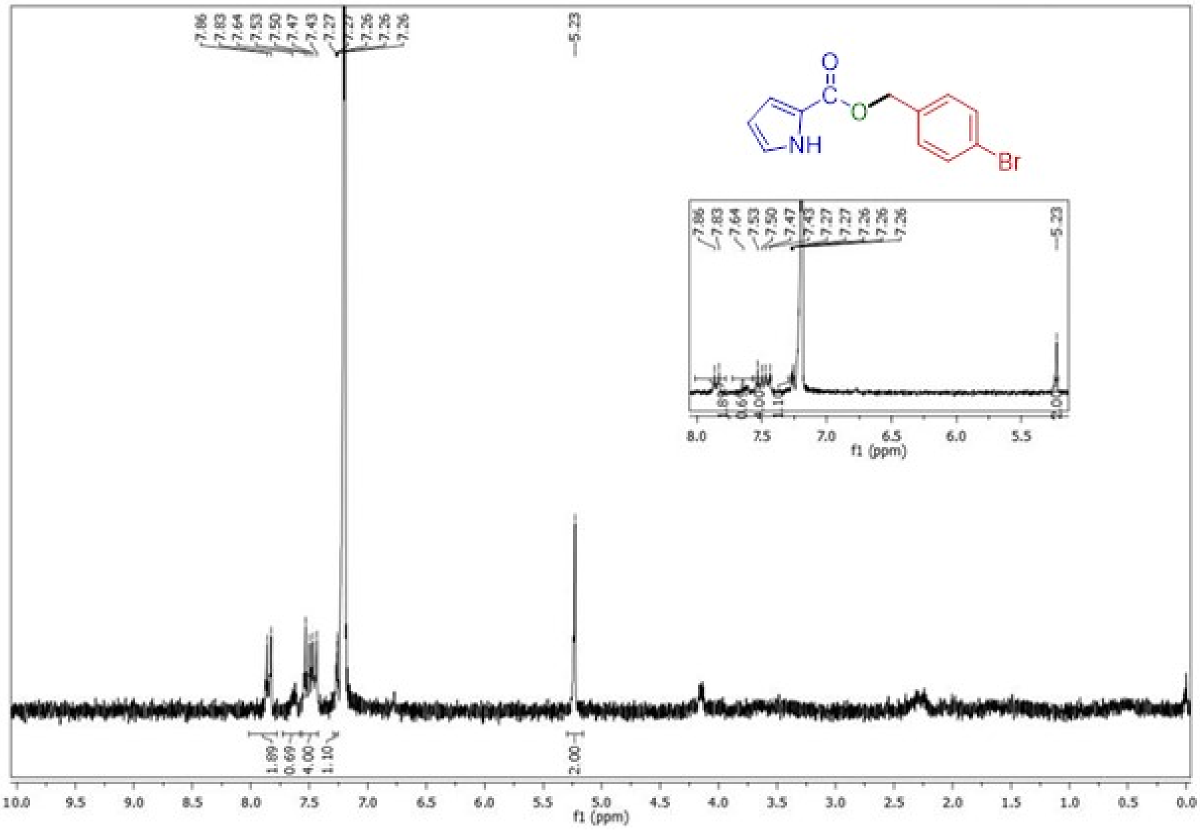

^{1}H-NMR of **3t**

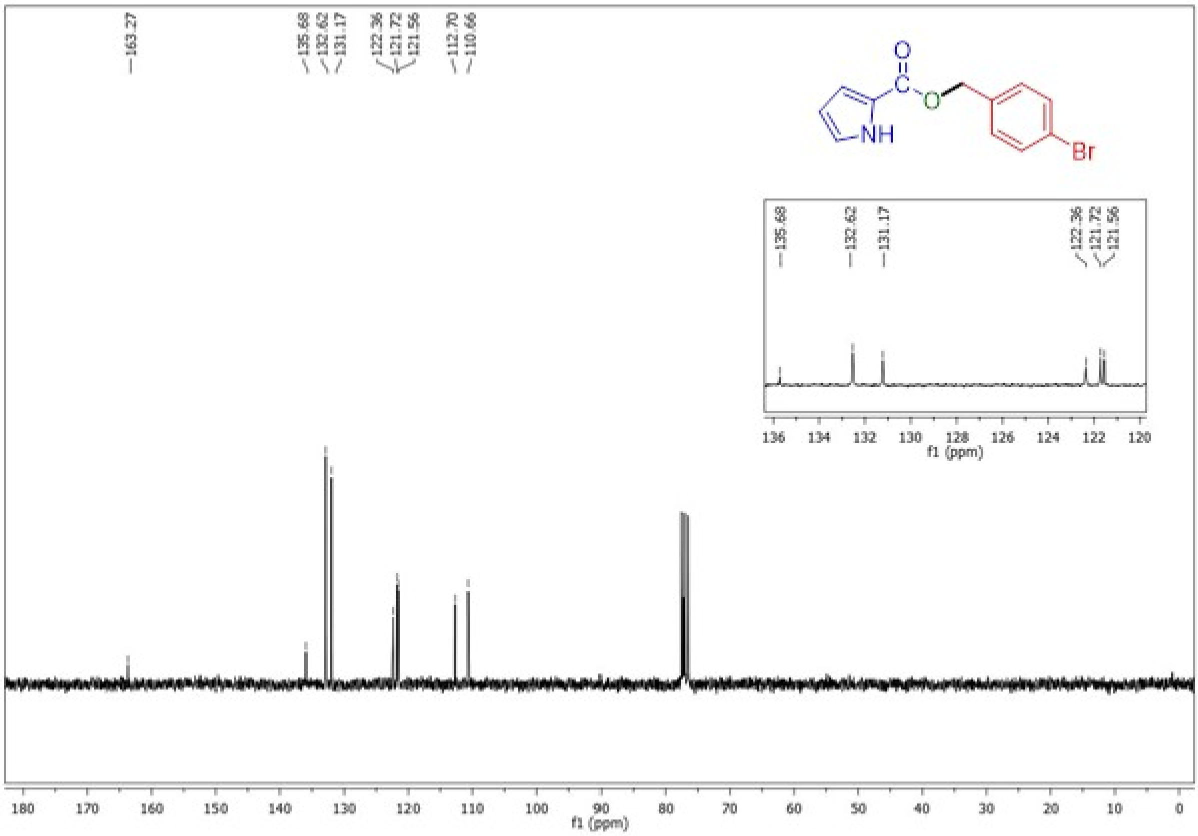

^{13}C-NMR of **3t**

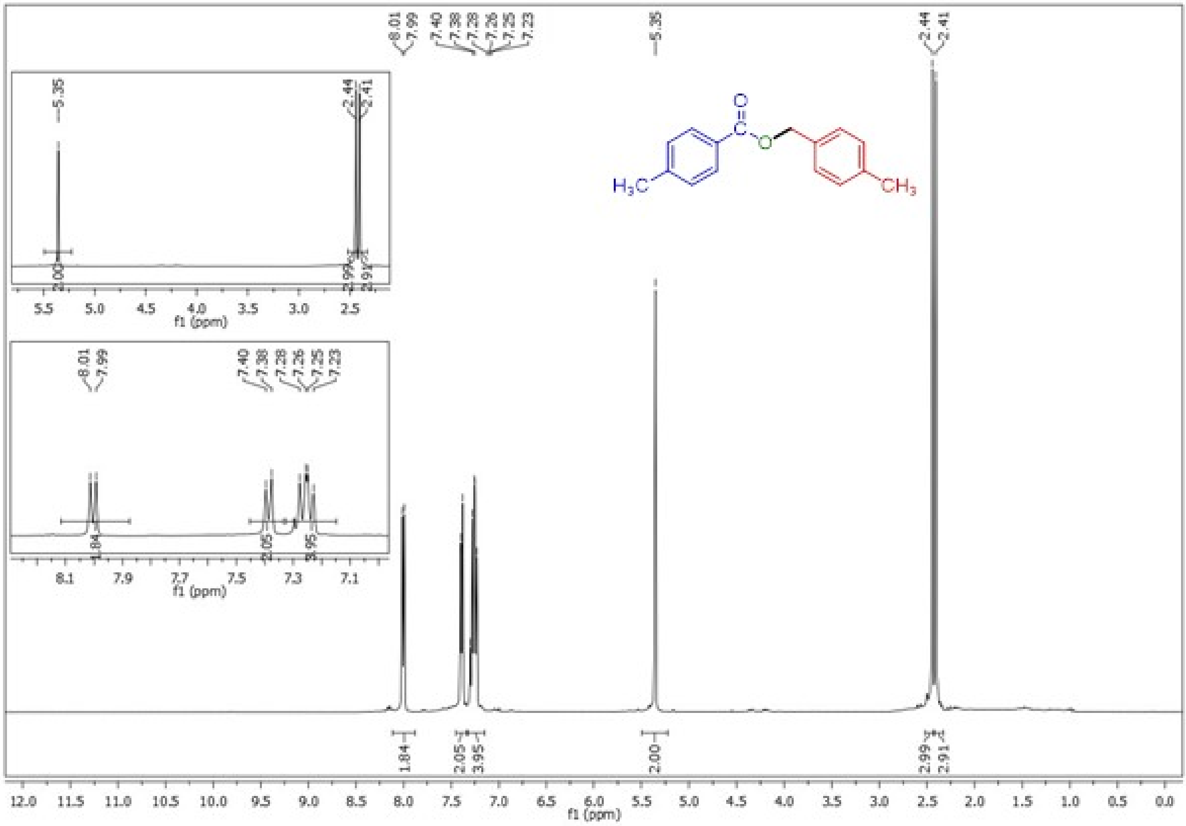

^{1}H-NMR of **3u**

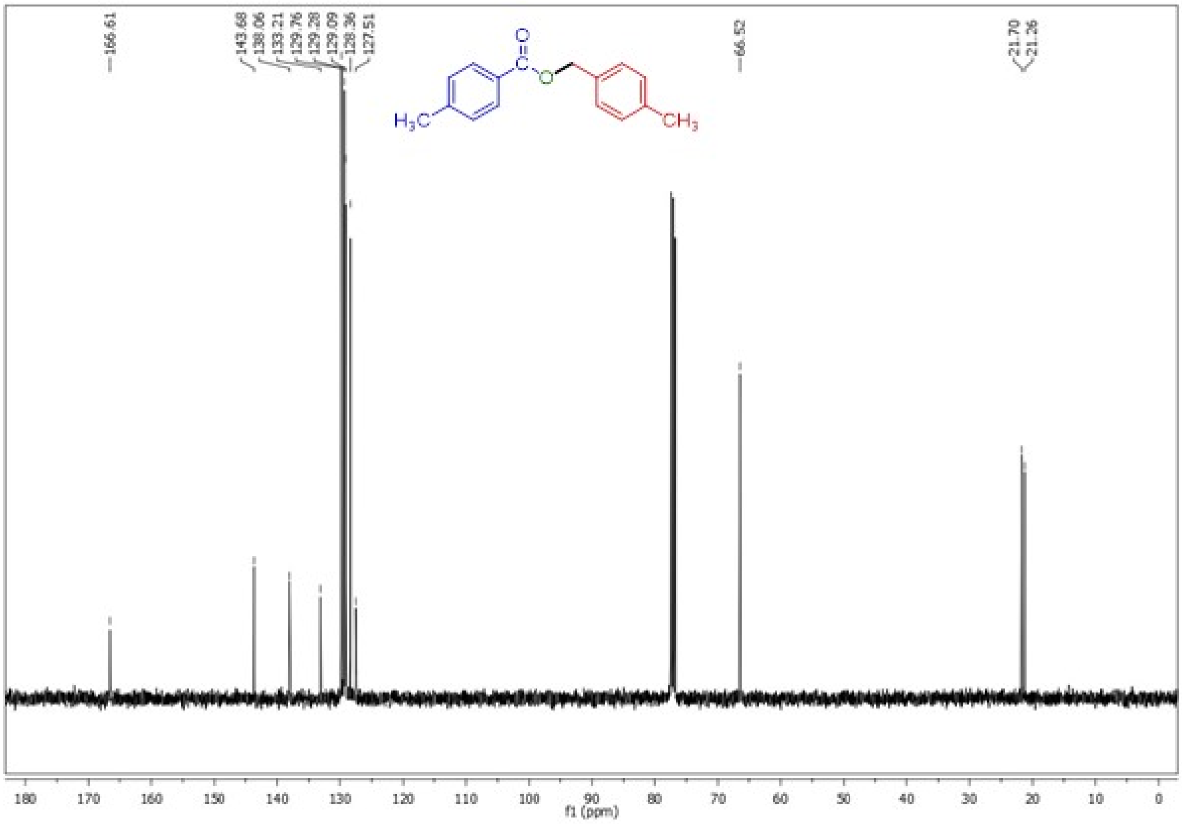

^{13}C-NMR of **3u**

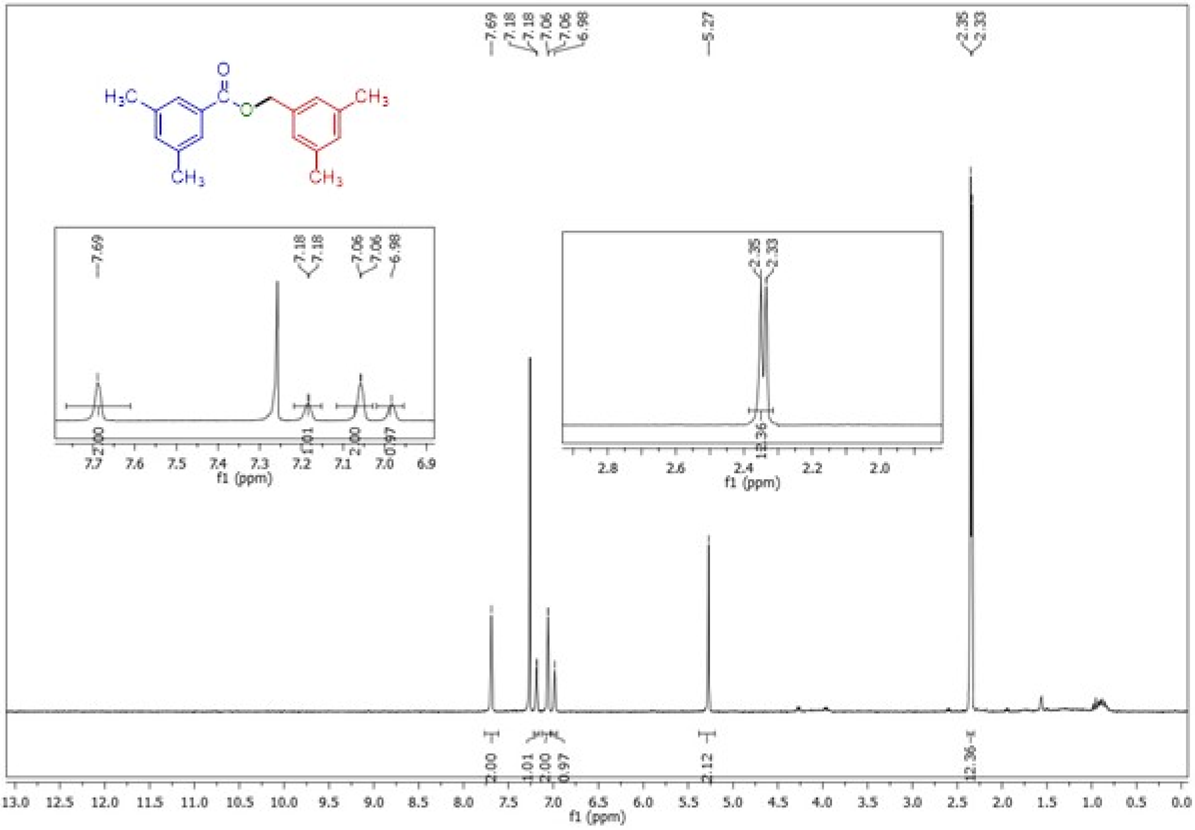

^{1}H-NMR of **3v**

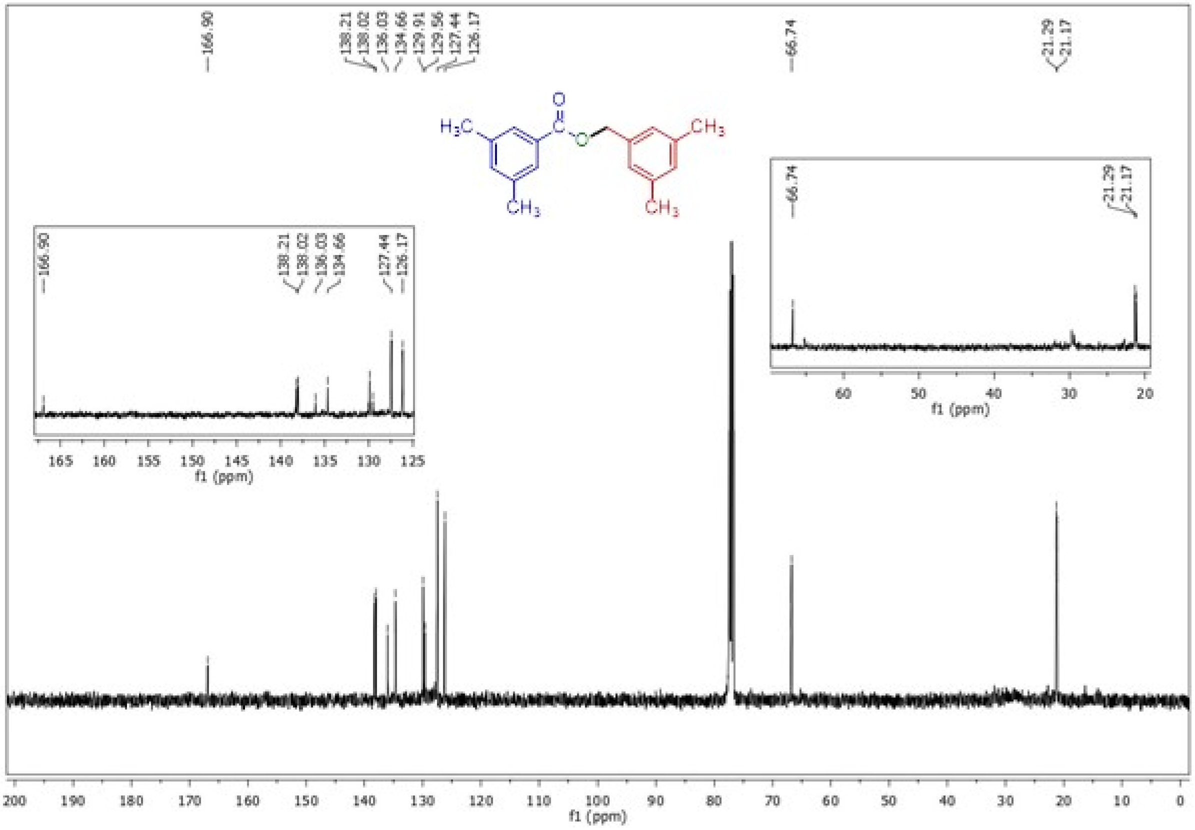

^{13}C-NMR of **3v**

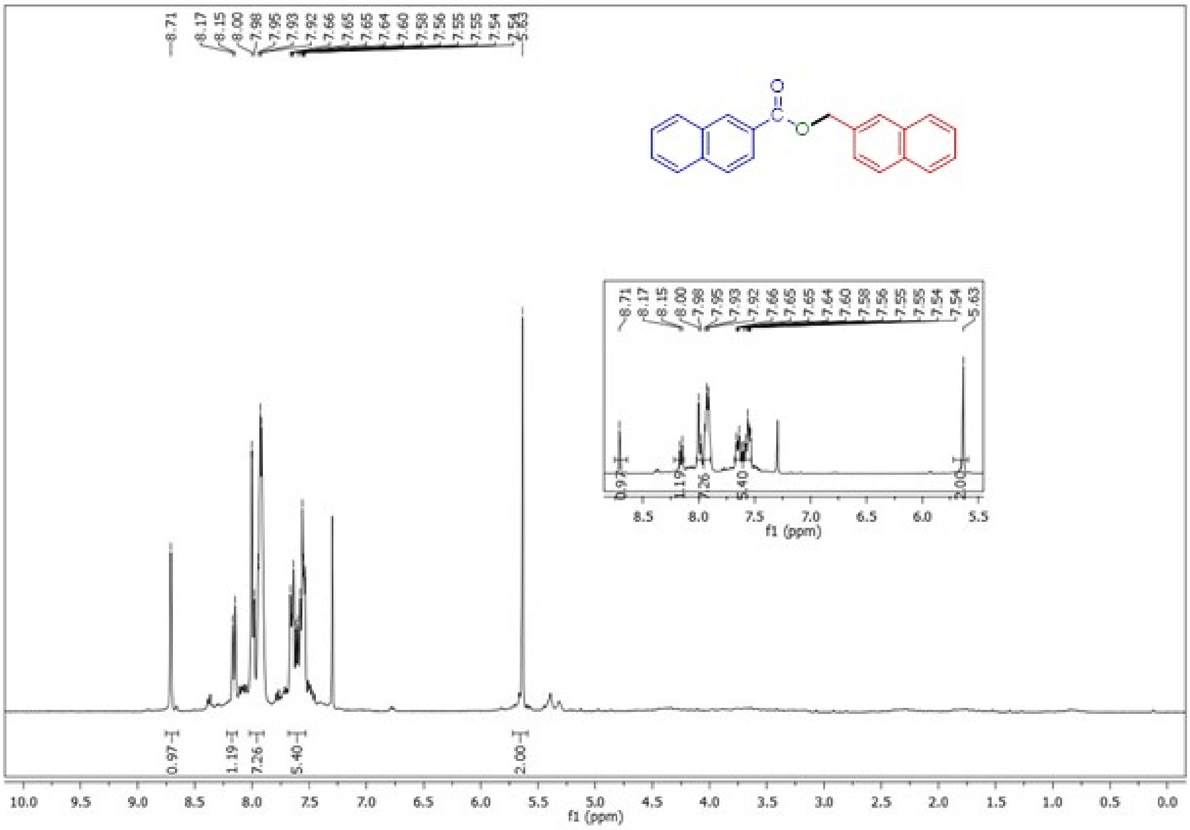

^{1}H-NMR of **3w**

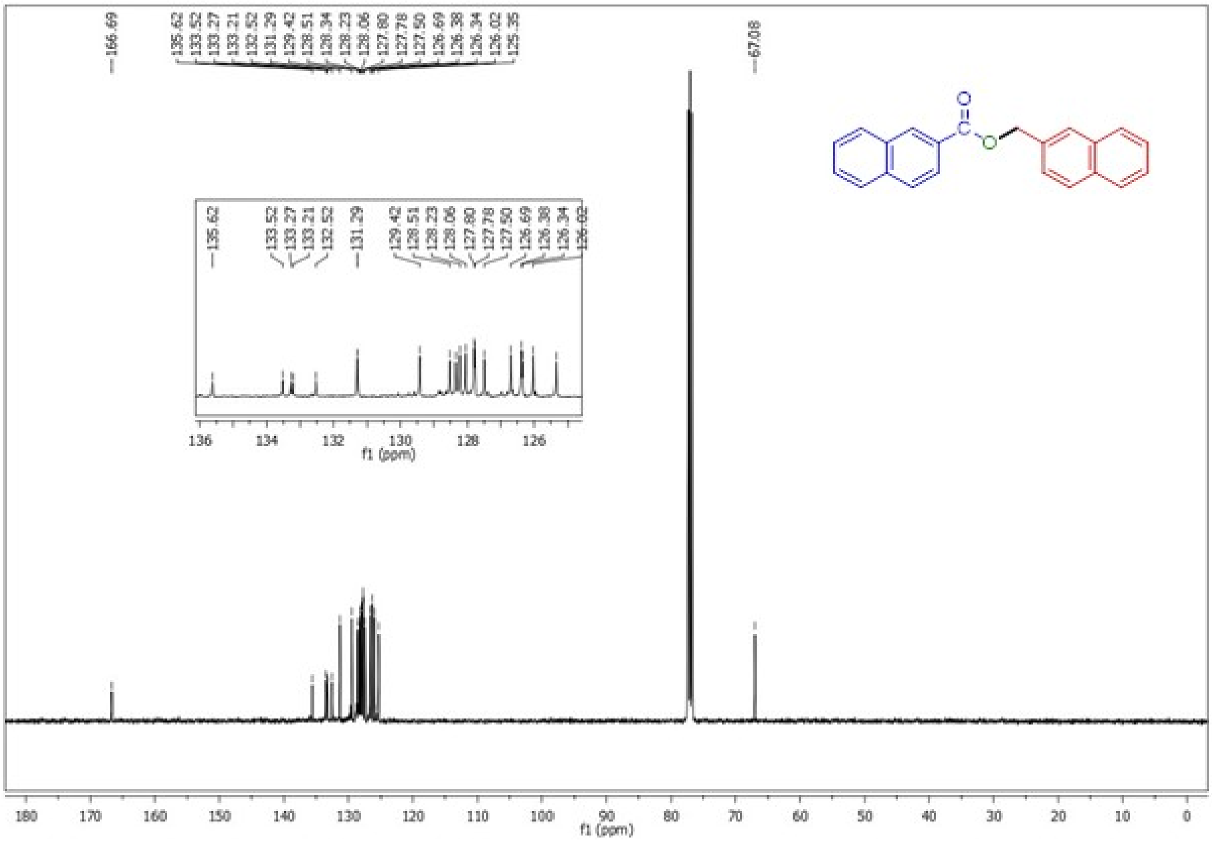

^{13}C-NMR of **3w**

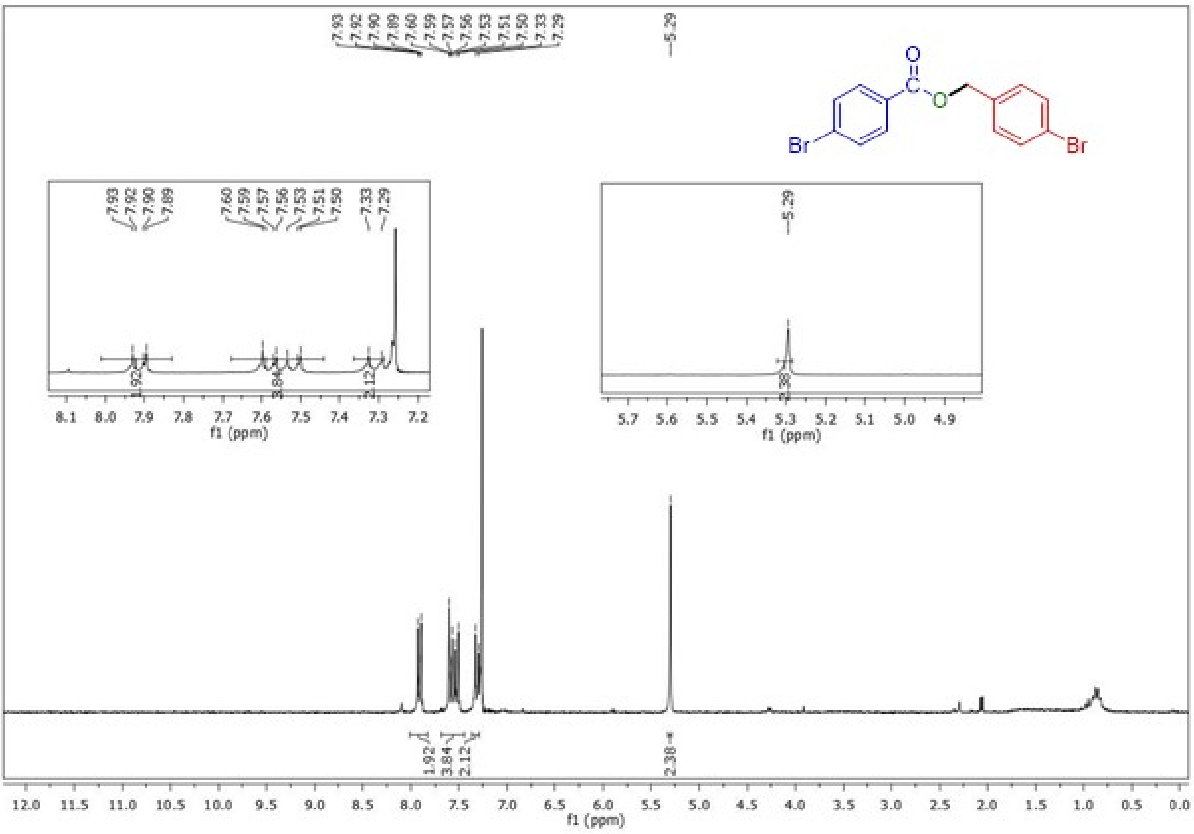

^{1}H-NMR of **3x**

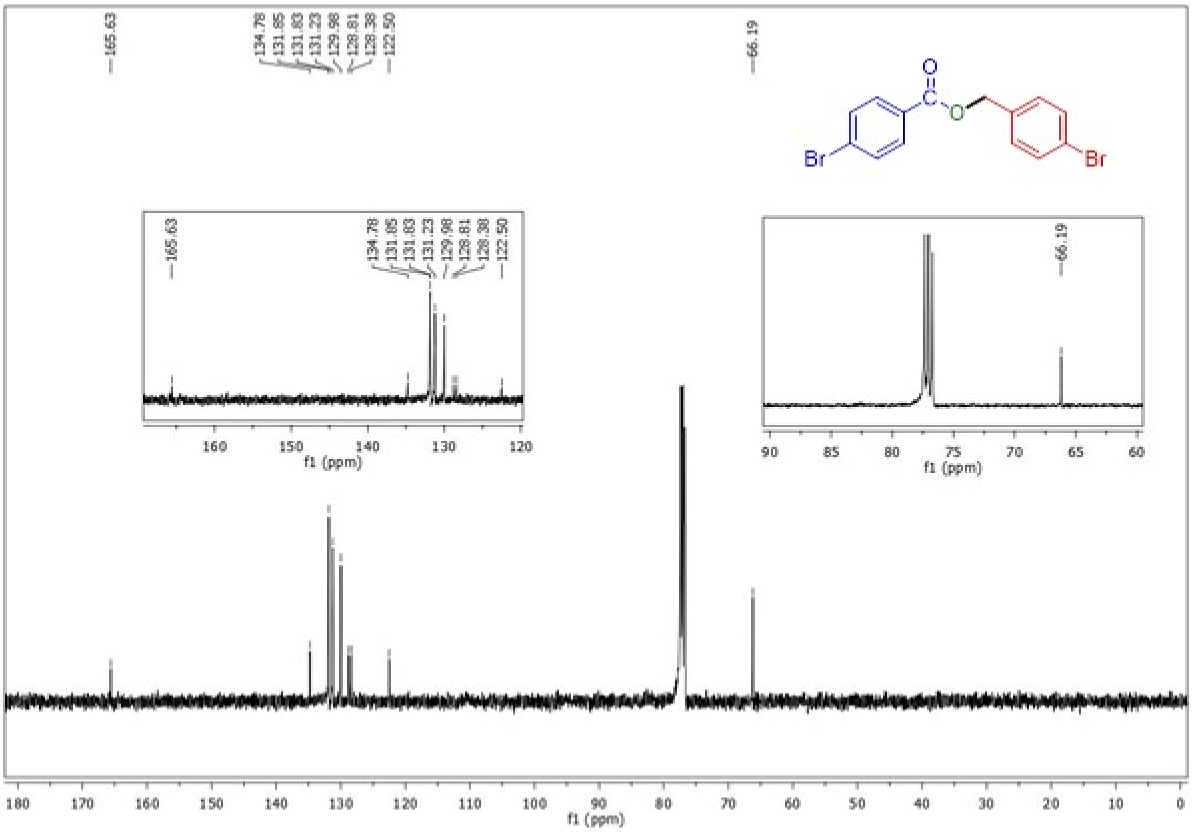

^{13}C-NMR of **3x**